MAIT cells promote inflammatory monocyte differentiation into dendritic cells during pulmonary intracellular infection

Anda I. Meierovics and Siobhán C. Cowley

Laboratory of Mucosal Pathogens and Cellular Immunology, Division of Bacterial, Parasitic, and Allergenic Products, Center for Biologics Evaluation and Research, U.S. Food and Drug Administration, Silver Spring, MD 20993

Mucosa-associated invariant T (MAIT) cells are a unique innate T cell subset that is necessary for rapid recruitment of activated CD4$^+$ T cells to the lungs after pulmonary *F. tularensis* LVS infection. Here, we investigated the mechanisms behind this effect. We provide evidence to show that MAIT cells promote early differentiation of CCR2-dependent monocytes into monocyte-derived DCs (Mo-DCs) in the lungs after *F. tularensis* LVS pulmonary infection. Adoptive transfer of Mo-DCs to MAIT cell–deficient mice (MR1$^{-/-}$ mice) rescued their defect in the recruitment of activated CD4$^+$ T cells to the lungs. We further demonstrate that MAIT cell–dependent GM-CSF production stimulated monocyte differentiation in vitro, and that in vivo production of GM-CSF was delayed in the lungs of MR1$^{-/-}$ mice. Finally, GM-CSF–deficient mice exhibited a defect in monocyte differentiation into Mo-DCs that was phenotypically similar to MR1$^{-/-}$ mice. Overall, our data demonstrate that MAIT cells promote early pulmonary GM-CSF production, which drives the differentiation of inflammatory monocytes into Mo-DCs. Further, this delayed differentiation of Mo-DCs in MR1$^{-/-}$ mice was responsible for the delayed recruitment of activated CD4$^+$ T cells to the lungs. These findings establish a novel mechanism by which MAIT cells function to promote both innate and adaptive immune responses.

INTRODUCTION

A fundamental function of the innate immune system is to activate adaptive immune responses critical for pathogen eradication. In many infection models, accumulation of Ly6C^{hi} CD11b$^+$ monocytes at the site of infection is an essential part of this process (Serbina et al., 2008). These cells are commonly referred to as inflammatory monocytes and express CCR2, a chemokine receptor that promotes emigration of cells from the bone marrow (Serbina and Pamer, 2006). Correspondingly, CCR2$^{-/-}$ mice are highly susceptible to numerous microbial infections because CCR2$^+$ Ly6C^{hi} CD11b$^+$ monocytes fail to exit the bone marrow and traffic to the site of infection (Serbina and Pamer, 2006; Serbina et al., 2008).

A critical role for CCR2$^+$ inflammatory monocytes in immune defense is their ability to differentiate into monocyte-derived DCs (Mo-DCs) at the site of infection (Peters et al., 2001; Hohl et al., 2009; Nakano et al., 2009; Osterholzer et al., 2009; Espinosa et al., 2014). Mo-DCs are typically characterized as Ly6C^{hi} CD11b^{hi} MHCII$^+$ CD11c^{int} cells and possess several important functions. In some infection models, such as *Listeria monocytogenes*, Mo-DCs include a subset of specialized TNF and inducible nitric oxide synthase–producing DCs (Tip-DCs) that express antimicrobial effector functions (Serbina et al., 2003; Tezuka et al., 2007). However, a large body of evidence also implicates Mo-DCs in the initiation of adaptive CD4$^+$ T cell responses to a variety of pathogens, including *Mycobacteria tuberculosis* (Peters et al., 2001, 2004), *Aspergillus fumigatus* (Hohl et al., 2009), *Histoplasma capsulatum* (Wüthrich et al., 2012), and *Leishmania major* (León et al., 2007). In the *A. fumigatus* pulmonary infection model, Mo-DCs transported antigen from the lungs to the draining lymph nodes, suggesting a possible mechanism by which they promote CD4$^+$ T cell priming (Hohl et al., 2009). Thus, the differentiation of inflammatory monocytes into Mo-DCs is likely an important step required for the initiation of CD4$^+$ T cell responses. Although in vivo and in vitro studies have shown that GM-CSF and M-CSF influence the differentiation of inflammatory monocytes into Mo-DCs (Kang et al., 2008; Bosschaerts et al., 2010; Chong et al., 2011; Greter et al., 2012; Chen et al., 2016), the cell types required to direct Mo-DC differentiation during infection have not been extensively investigated.

Although conventional CD4$^+$ T cells respond slowly and require signals from specialized DCs for activation, innate-like T cells respond more quickly to infectious assaults, uniquely positioning them to influence early innate events. Mucosa-associated invariant T (MAIT) cells are a subset of innate-like T cells that express an evolutionarily conserved T cell receptor α chain restricted by the nonpolymorphic MHC class I–related protein (MR1; Huang et al., 2005, 2009; Gold and Lewinsohn, 2013). MAIT cells are activated by microbial

Correspondence to Siobhán C. Cowley: siobhan.cowley@fda.hhs.gov

Abbreviations used: LVS, live vaccine strain; MAIT, mucosa-associated invariant T; Mo-DC, monocyte-derived DC; MR1, MHC class I–related protein.

The Rockefeller University Press $30.00
J. Exp. Med. 2016 Vol. 213 No. 12 2793–2809
https://doi.org/10.1084/jem.20160637

riboflavin metabolite-derived antigens presented by MR1, distinguishing them from all other αβ T cells (Kjer-Nielsen et al., 2012). Because the riboflavin biosynthetic pathway is unique to microbes, these metabolites are comparable to microbial molecular patterns, indicating that MAIT cells likely participate in early pattern-recognition surveillance. Indeed, MAIT cells quickly secrete IFN-γ, TNF, IL-17, and cytotoxic effector mechanisms when stimulated with a wide variety of pathogens in vitro (Gold et al., 2010; Le Bourhis et al., 2013; Cowley, 2014; Cui et al., 2015). The in vivo importance of MAIT cells is evident in MR1$^{-/-}$ mice, which lack MAIT cells and are impaired in their ability to control infections with *Francisella tularensis*, *Mycobacterium bovis* BCG, and *Klebsiella pneumoniae* (Georgel et al., 2011; Chua et al., 2012; Meierovics et al., 2013). However, thus far little is known about the activities that MAIT cells contribute to the in vivo generation of protective innate and adaptive immune responses.

F. tularensis is a Gram negative, facultative intracellular bacterium and the causative agent of tularemia. Classified as a Tier 1 bioterrorism agent, inhalation of virulent strains of *F. tularensis* rapidly progresses to acute lethal disease in up to 60% of untreated patients (Ellis et al., 2002). The attenuated *F. tularensis* live vaccine strain (LVS) has shown potential as a protective vaccine in animal studies, and has been used as an investigational product in the United States (Dennis et al., 2001). Although avirulent for humans, *F. tularensis* LVS causes a fulminant pulmonary infection in mice, with an i.n. LD_{50} of ~10^3–10^4 bacteria (Elkins et al., 2003). Importantly, i.n. infection of mice with sublethal doses of *F. tularensis* LVS results in the recruitment of large numbers of MAIT cells to the lungs and offers a convenient platform to study pulmonary MAIT cell immune responses (Meierovics et al., 2013).

We have previously used the *F. tularensis* LVS murine pulmonary infection model to probe the role of MAIT cells in mucosal immune responses, demonstrating that accumulation of activated CD4$^+$ T cells in the lungs of MR1$^{-/-}$ mice was delayed after respiratory LVS infection (Meierovics et al., 2013). Similar to other intracellular pathogens, optimal defense against LVS infection requires conventional CD4$^+$ and/or CD8$^+$ T cells for clearance, and, correspondingly, MR1$^{-/-}$ mice exhibited increased susceptibility and delayed clearance of a sublethal LVS pulmonary infection (Yee et al., 1996; Meierovics et al., 2013). We were therefore interested in determining the mechanisms by which MAIT cells influence early activation and/or recruitment of conventional T cells. Here, we show that MR1$^{-/-}$ mice exhibit delayed differentiation of CCR2–dependent inflammatory monocytes (defined as Ly6C^{hi}CD11b$^+$ cells) into Mo-DCs (generally defined as Ly6C^{hi}CD11b$^+$CD11c$^+$MHCII$^+$ cells) after pulmonary *F. tularensis* LVS infection, and that this early defect impairs the accumulation of activated CD4$^+$ T cells in the lungs. We further demonstrate that MAIT cells contribute to early GM-CSF production, and that GM-CSF is necessary for Mo-DC accumulation during LVS pulmonary infection. These findings reveal a previously unappreciated role for MAIT cells in the promotion of inflammatory monocyte differentiation and the development of DCs that facilitate later adaptive immune responses.

RESULTS

Early accumulation of CCR2-dependent CD11b$^+$ DCs in the lungs of MR1$^{-/-}$ mice is impaired after pulmonary mucosal infection

To determine whether MAIT cells influence early inflammatory events during in vivo pulmonary infection, we examined myeloid cell numbers in the lungs after sublethal i.n. *F. tularensis* LVS infection. Inflammatory myeloid cells in the lungs possess a heterogeneous phenotype, and discrimination of DCs from macrophages requires a complex gating strategy (Sköld and Behar, 2008; Hohl et al., 2009). Lung cells harvested from WT and MR1$^{-/-}$ mice on day 4 after sublethal i.n. LVS infection were first analyzed for CD11c and MHC class II expression, and subsequently divided into CD103$^+$ intraepithelial DCs (gate R1), macrophages (gate R2), or CD11b$^+$ DCs (gate R3) in accordance with previously published studies (Fig. 1 A; Sung et al., 2006; Hohl et al., 2009). As compared with WT mice, MR1$^{-/-}$ mice had a lower proportion of CD11c$^+$ MHCII$^+$ cells in their lungs on day 4 after infection (Fig. 1 A). Accumulation of CD11b$^+$ DCs, but not CD103$^+$ DCs or macrophages, was observed in the lungs of WT mice on days 3, 4, and 5 after sublethal i.n. LVS infection (Fig. 1, A and B). In contrast, MR1$^{-/-}$ mice failed to accumulate CD11b$^+$ DCs at the same rate as their WT counterparts, with significantly fewer CD11b$^+$ DCs present in their lungs at days 4 and 5 after infection. In keeping with studies performed in other pulmonary infection models (Hohl et al., 2009; Osterholzer et al., 2009), recruitment of CD11b$^+$ DCs to the lungs after i.n. LVS infection was dependent on CCR2 signaling, as CCR2$^{-/-}$ mice had reduced numbers of CD11b$^+$ DCs in their lungs on day 4 after sublethal i.n. LVS infection as compared with WT mice (Fig. 1, A and C). Importantly, the severe defect in accumulation of CD11b$^+$ DCs in the lungs of CCR2$^{-/-}$ mice was not significantly different from that of MR1$^{-/-}$ mice on day 4 after infection (Fig. 1 C). Overall, these data demonstrate that mice lacking MAIT cells fail to accumulate a CCR2-dependent population of CD11b$^+$ DCs in their lungs at the same rate as their WT counterparts.

We further characterized the CD11b$^+$ DC population in the lungs of WT mice to gain insight into their function. As shown in Fig. 2 (A and B), CD11b$^+$ DCs from the lungs of WT mice 4 d after i.n. LVS infection were highly positive for the co-stimulatory molecules CD86 and CD40 (~93 and 94%, respectively). Approximately 13% of CD11b$^+$ DCs expressed the chemokine receptor CCR7, which is known to facilitate lymph node migration. CD11b$^+$ DCs expressed CD172α, CD64, Ly6C, F4/80, and CD24, consistent with inflammatory CD11b$^+$ DCs that have been described in other infection models (Greter et al., 2012; Guilliams et al., 2013). In contrast, CD11b$^+$ DCs expressed low levels of two markers

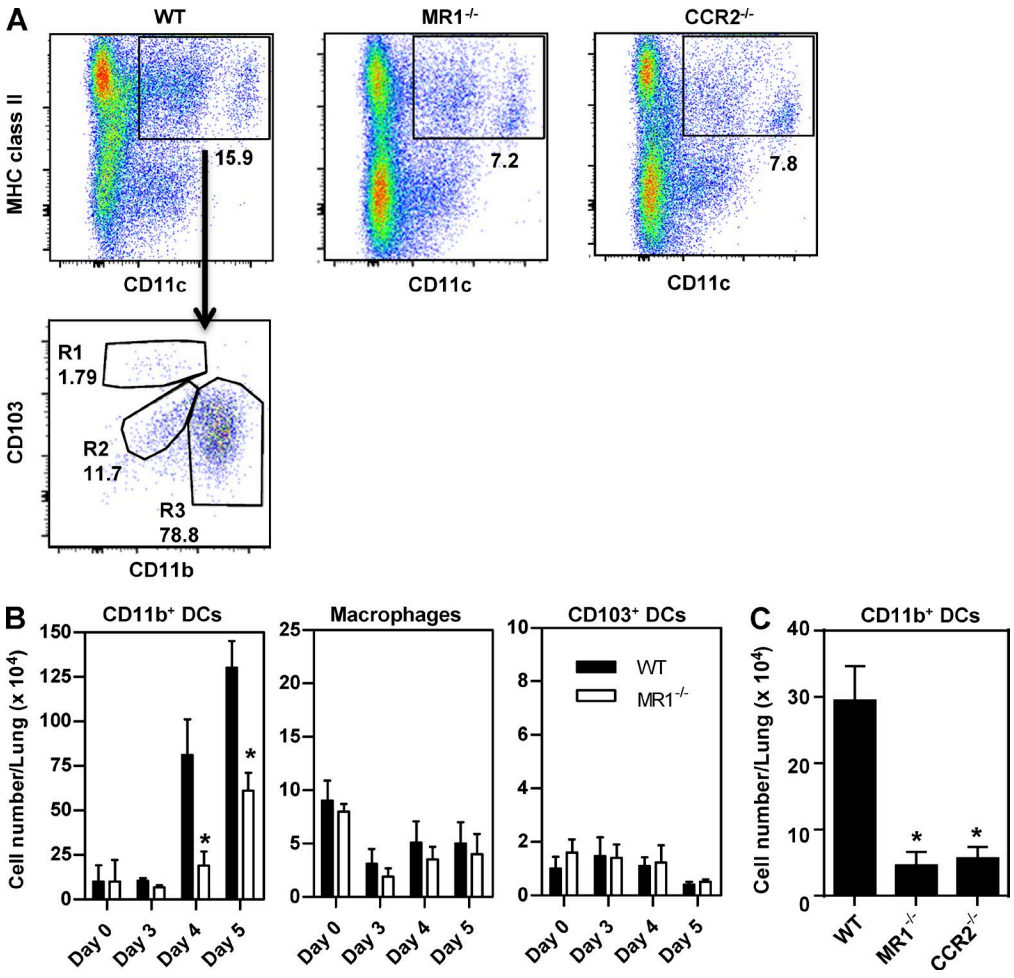

Figure 1. **Accumulation of CCR2-dependent CD11b$^+$ DCs in the lungs of MR1$^{-/-}$ mice is impaired after *F. tularensis* i.n. LVS infection.** Wild-type C57BL/6, MR1$^{-/-}$, and CCR2$^{-/-}$ mice were i.n. infected with a sublethal dose of 2 × 10^2 CFU *F. tularensis* LVS, and total lung cells were harvested at the indicated time points after infection to evaluate the presence of myeloid cells. (A) Representative flow cytometry dot plots of lung cells on day 4 after infection, demonstrating the gating scheme used to identify CD103$^+$ DCs (gate R1), macrophages (gate R2), and CD11b$^+$ DCs (gate R3). (B) Accumulation of CD103$^+$ DCs, macrophages, and CD11b$^+$ DCs in the lungs of WT mice after i.n. LVS infection. (C) Total numbers of CD11b$^+$ DCs in the lungs of WT, MR1$^{-/-}$, and CCR2$^{-/-}$ mice on day 4 after i.n. LVS infection. All data are representative of three independent experiments (n = 5 mice per group) and are the mean ± SEM. *, P < 0.01, compared with LVS-infected WT mice at the same time point. Data were analyzed via one-way ANOVA, followed by the Student-Newman-Keuls multiple stepwise comparison.

consistent with resident DCs, B220, and CD8α (~5 and <1%, respectively). Of note, the CD11b$^+$ DC population expressed CSF-2Rα (GM-CSF receptor; 98%), but not CSF-1R (M-CSF receptor, or CD115; 8%). To determine whether these cells possess DC morphology, CD11b$^+$ DCs were flow sorted from the lungs of WT mice on day 4 after i.n. LVS infection, and examined by microscopy. The CD11b$^+$ DC population exhibited morphological variation, although many cells possessed characteristics consistent with DCs, such as typical dendrites (Fig. 2 C).

CD11b$^+$ DCs are derived from recently recruited, CCR2-dependent, inflammatory monocytes (defined as Ly6C^{hi} CD11b$^+$ cells; Lin et al., 2008; Sköld and Behar, 2008; Hohl et al., 2009; Osterholzer et al., 2009; Shi and Pamer, 2011). As noted in the previous paragraph, the CD11b$^+$ DC population identified in the lungs of infected WT mice was predominantly Ly6C$^+$ (94%), and dependent on CCR2 for their accumulation in the lungs, consistent with the proposal that they are derived from recently recruited inflammatory Ly6C^{hi} CD11b$^+$ monocytes (Figs. 1 and 2 A). Because co-expression of CD11c and MHCII by inflammatory Ly6C^{hi} CD11b$^+$ monocytes is frequently used to identify inflammatory monocyte–derived DCs (Mo-DCs; Guilliams et al., 2009; Bosschaerts et al., 2010), we used flow cytometry to determine whether the CD11b$^+$ DC population are classical Mo-DCs. As shown in Fig. 2 D, flow cytometry analysis confirmed that Mo-DCs in WT mice reside entirely within the CD11b$^+$ DC population, demonstrating that CD11b$^+$ DCs and Mo-DCs are one and the same. Hereafter, we will refer to these cells as Mo-DCs.

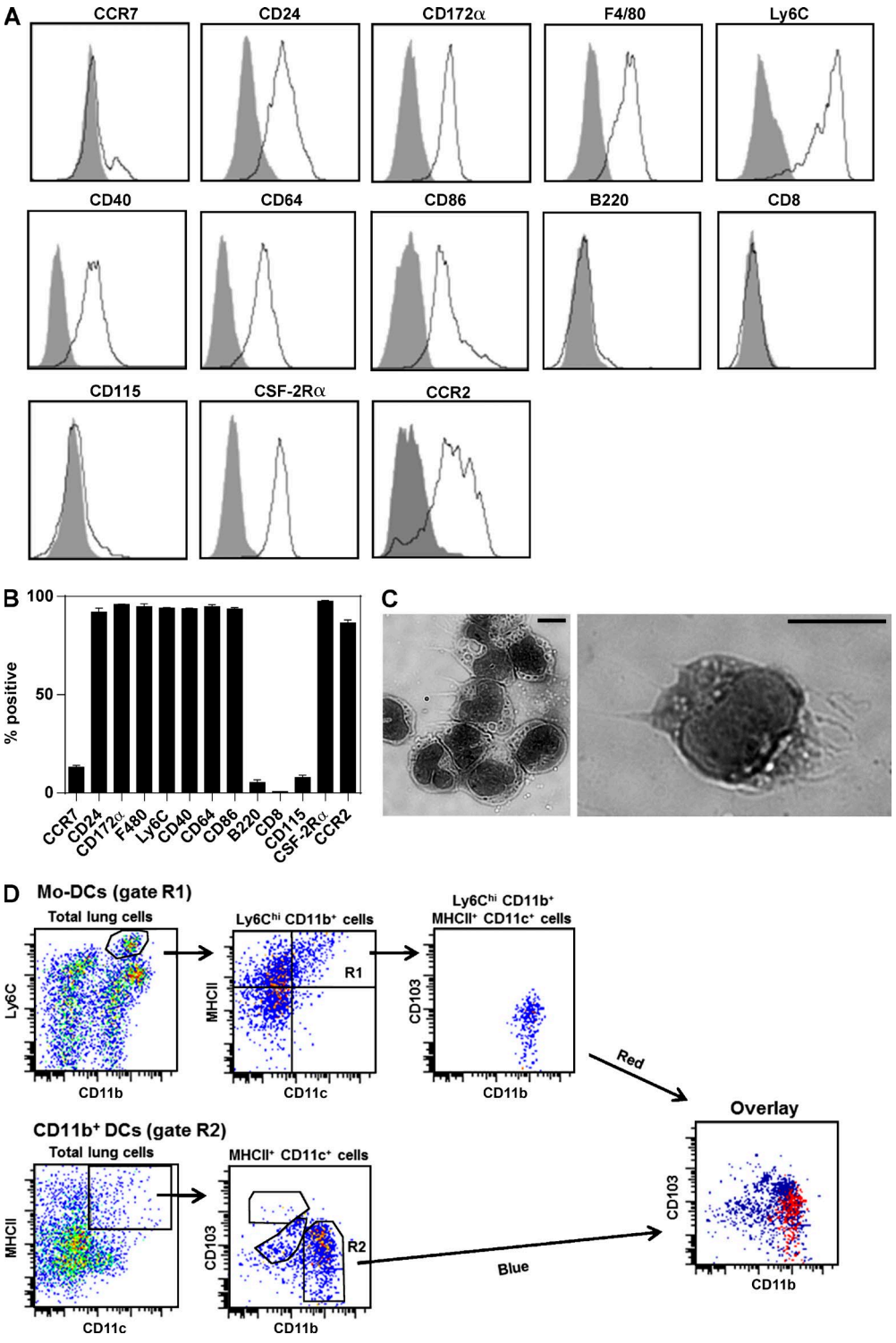

Figure 2. **Characterization of CD11b$^+$ DCs in the lungs of mice after i.n. *F. tularensis* LVS infection.** Wild-type C57BL/6 mice were infected with a sublethal dose of 2×10^2 CFU *F. tularensis* i.n. LVS, and total lung cells were harvested on day 4 after infection. (A) Expression of myeloid cell markers by CD11b$^+$ DCs. In the flow cytometry histograms shown, CD11b$^+$ DCs were first gated as indicated in Fig. 1 A, gate R3. Gray histogram shows fluorescence minus one control, and white histogram shows staining by the indicated antibody. Data are representative of two independent experiments ($n = 3$ mice per group). (B) Quantitation of myeloid marker expression by lung CD11b$^+$ DCs (based on percentage of positive cells). Data are representative of two independent experiments ($n = 3$ mice per group). (C) Cytospin preparations of CD11b$^+$ DCs purified from the lungs of 10 LVS-infected WT mice on day 4 after infection by fluorescence-activated cell sorting and examined by light microscopy. Bars, 10 µm. Data are representative of two independent experiments.

MAIT cells are required for the early differentiation of inflammatory monocytes into Mo-DCs in vivo

We next investigated the reason for the reduced accumulation of Mo-DCs in the lungs of MR1$^{-/-}$ mice during i.n. LVS infection. To determine whether the diminished number of Mo-DCs in the lungs of MR1$^{-/-}$ mice is a consequence of reduced recruitment of their inflammatory monocyte precursors, we compared Ly6C^{hi} CD11b^{+} monocytes in the lungs of WT, CCR2$^{-/-}$, and MR1$^{-/-}$ mice after i.n. LVS infection. As shown in Fig. 3 A, the total numbers and percentages of Ly6C^{hi} CD11b^{+} monocytes in the lungs of MR1$^{-/-}$ and WT mice were not significantly different on day 4 after infection. In contrast, Ly6C^{hi} CD11b^{+} monocytes in the lungs of CCR2$^{-/-}$ mice were significantly reduced as compared with WT and MR1$^{-/-}$ mice. Because CCR2 facilitates egress of Ly6C^{hi} CD11b^{+} monocytes from the bone marrow, we examined the percentage of these cells present in the bone marrow of WT, CCR2$^{-/-}$, and MR1$^{-/-}$ mice after i.n. LVS infection. CCR2$^{-/-}$ mice significantly accumulated high levels of Ly6C^{hi} CD11b^{+} monocytes in the bone marrow compared with WT mice; however, consistent with the normal recruitment of Ly-6C^{hi} CD11b^{+} monocytes to the lungs of MR1$^{-/-}$ mice, bone marrow from these mice did not accumulate Ly6C^{hi} CD11b^{+} monocytes during the first 4 d after infection (Fig. 3 B). Overall, these results demonstrate that recruitment of Ly6C^{hi} CD11b^{+} monocytes to the lungs of mice after LVS infection requires CCR2. Further, MR1$^{-/-}$ mice were not defective in the emigration of Ly6C^{hi} CD11b^{+} monocytes from the bone marrow and their subsequent recruitment to the lungs.

Because MR1$^{-/-}$ mice were defective in Mo-DC accumulation (Fig. 1 B), but not in the recruitment of their precursor cells to the lungs (Ly6C^{hi} CD11b^{+} monocytes; Fig. 3 A), we investigated the differentiation of Ly6C^{hi} CD11b^{+} monocytes into Mo-DCs in these mice. Inflammatory Ly6C^{hi} CD11b^{+} monocytes that differentiate into Mo-DCs in response to infection up-regulate CD11c, MHC II, and a variety of co-stimulatory molecules (CD40, CD80, and CD86; Hohl et al., 2009; Osterholzer et al., 2009). To assess differentiation of inflammatory monocytes into Mo-DCs during infection, we examined coexpression of MHCII and CD11c by Ly6C^{hi} CD11b^{+} monocytes in the lungs of WT mice and MR1$^{-/-}$ mice on days 3, 4, and 5 after i.n. LVS infection. Only a very small number of Ly-6C^{hi} CD11b^{+} monocytes in WT and MR1$^{-/-}$ mice co-stained for MHCII and CD11c on day 3 after infection (Fig. 4 A). However, by days 4 and 5 after infection, the number of Ly-6C^{hi} CD11b^{+} monocytes coexpressing MHCII and CD11c significantly increased in WT mice; in contrast, the numbers of Ly6C^{hi} CD11b^{+} monocytes coexpressing CD11c and MHCII were significantly lower in MR1$^{-/-}$ mice as compared with WT mice (Fig. 4, A and B). Because day 4 after infection was the critical time at which Mo-DCs began to accumulate in the lungs, we compared the percentage of Ly6C^{hi} CD11b^{+} monocytes expressing MHCII, CD11c, and CD86 in WT and MR1$^{-/-}$ mice on day 4 after i.n. LVS infection. As shown in Fig. 4 C, there were significantly fewer Ly6C^{hi} CD11b^{+} monocytes in MR1$^{-/-}$ mice expressing MHCII, CD11c, and CD86 as compared with their WT counterparts. The Ly6C^{hi} CD11b^{+} monocytes of MR1$^{-/-}$ mice exhibited a 62 $\pm$ 8% and 65 $\pm$ 5% reduction in expression of CD11c and CD86 as compared with WT mice, respectively, whereas expression of MHCII was reduced by 37 $\pm$ 8%. Overall, these data demonstrate that early differentiation of inflammatory monocytes into Mo-DCs in the lungs is impaired in the absence of MAIT cells.

We next investigated whether the differentiation of inflammatory monocytes into Mo-DCs resulted in a change in cell morphology consistent with DCs. To this end, we purified the CD11c^{+} and CD11c^{-} populations of Ly6C^{hi} CD11b^{+} monocytes from WT mice on day 4 after i.n. LVS infection. As shown in Fig. 4 D, CD11c^{+} Ly6C^{hi} CD11b^{+} cells exhibited a mixed phenotype that included cells with characteristic DC morphology, including surface projections and numerous cytoplasmic vacuoles, as well as some round cells lacking clear dendrites. In contrast, Ly6C^{hi} CD11b^{+} cells that lacked CD11c expression exhibited few cells with dendritic morphology and instead consisted of round cells with pronounced surface blebs and vacuoles, consistent with monocytes (Fig. 4 D). To further assess whether acquisition of CD11c expression coincided with LVS uptake, we performed flow cytometry on lung cells harvested from WT mice on day 4 after infection with an LVS strain expressing GFP (LVS-GFP). We compared these cells to those obtained from mice infected with nonfluorescent LVS to assess background fluorescence. As shown in Fig. 4 (E and F), only a small number of cells in the CD11c^{-} subset of Ly6C^{hi} CD11b^{+} cells harbored LVS-GFP (~0–2% GFP^{+}); in contrast, the CD11c^{+} subset of Ly6C^{hi} CD11b^{+} cells contained cells that were positive for LVS-GFP (~5–8% GFP^{+}). Thus, inflammatory monocytes that have differentiated into Mo-DCs possess some dendritic morphology and contain cells harboring intracellular LVS, indicating that a subset of this population has the potential to present LVS antigen.

Mo-DCs rescue impaired CD4^{+} T cell activation and/or recruitment to the lungs in MR1$^{-/-}$ mice

In other infection models, Mo-DCs promote early priming of naive CD4^{+} T cells. Because MR1$^{-/-}$ mice exhibit delayed appearance of activated CD4^{+} T cells in the lungs during LVS pulmonary infection (Meierovics et al., 2013), we hypothesized that the reduced numbers of Mo-DCs

(D) Lung Mo-DCs and CD11b^{+} DCs are the same population by flow cytometry analysis. Wild-type C57BL/6 mice were infected with a sublethal dose of 2 × 10^{2} CFU *F. tularensis* i.n. LVS, and total lung cells were harvested on day 4 after infection to evaluate Mo-DCs and CD11b^{+} DCs. Representative dot plots of lung cells showing the gating scheme for Mo-DCs (gate R1) and CD11b^{+} DCs (gate R2). Overlay of the Mo-DC gating scheme is shown in red, and the CD11b^{+} DC gating scheme shown in blue. Data are representative of three independent experiments (n = 5 mice).

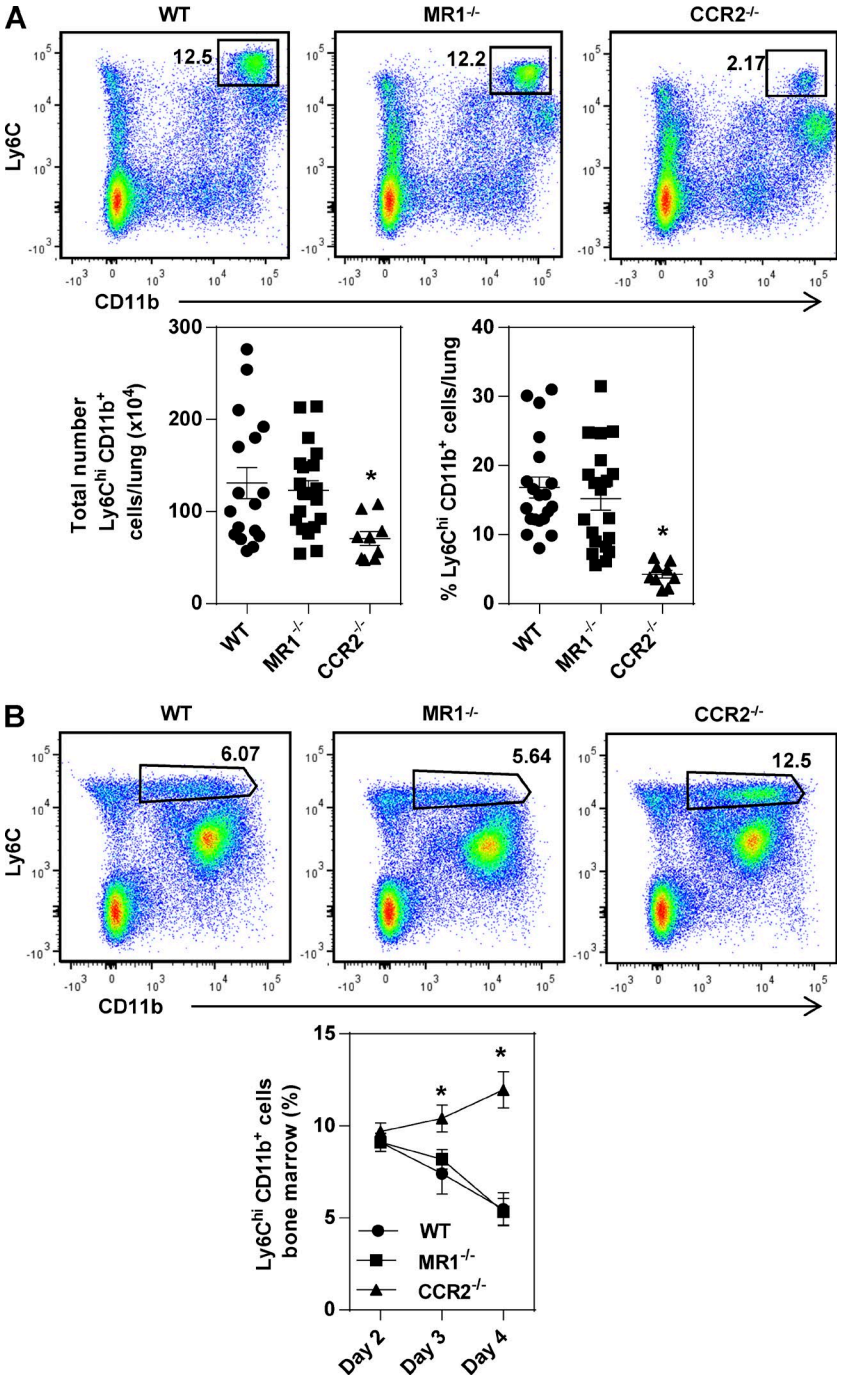

Figure 3. **Inflammatory monocyte recruitment to the lungs of MR1$^{-/-}$ mice is not impaired after i.n. *F. tularensis* LVS infection.** Wild-type C57BL/6, MR1$^{-/-}$, and CCR2$^{-/-}$ mice were i.n. infected with a sublethal dose of 2 × 10^2 CFU *F. tularensis* LVS, and (A) total lung cells were harvested on day 4 after infection to evaluate the presence of Ly6C^{hi} CD11b$^+$ inflammatory monocytes. Representative flow cytometry dot plots are shown, as well as enumeration of the total number of Ly6C^{hi} CD11b$^+$ inflammatory monocytes in the lungs of mice. Data are representative of four pooled experiments (n = 3–5 mice per group) and are the mean ± SEM. *, P < 0.01, compared with LVS-infected WT mice at the same time point. (B) Total bone marrow cells were harvested on day 4 after infection to evaluate the presence of Ly6C^{hi} CD11b$^+$ monocytes. Representative flow cytometry dot plots are shown, as well as the percentage of Ly-6C^{hi} CD11b$^+$ monocytes in the bone marrow of mice. Data are representative of three independent experiments (n = 5 mice per group) and are the mean ± SEM. *, P < 0.01, compared with LVS-infected WT mice at the same time point. Data were analyzed via one-way ANOVA, followed by the Student-Newman-Keuls multiple stepwise comparison.

in MR1$^{-/-}$ mice may contribute to this phenomenon. To test this hypothesis, Mo-DCs were purified by flow sorting from the lungs of WT mice on day 4 after infection, and adoptively transferred to MR1$^{-/-}$ mice late on day 3 after LVS infection. The appearance of activated (CD44$^+$ CD69$^+$) CD4$^+$ T cells was evaluated in the lungs of MR1$^{-/-}$ adoptive transfer recipients, mock-treated MR1$^{-/-}$ mice, and untreated WT mice on day 8 after i.n. LVS infection, when activated CD4$^+$ T cells first appear in the lungs. As shown in Fig. 5, mock-treated MR1$^{-/-}$ mice exhibited a significant 75% reduction in the number of activated CD4$^+$ T cells in the lungs as compared with WT mice. In contrast, adoptive transfer of Mo-DCs to MR1$^{-/-}$ mice significantly increased the numbers of activated CD4$^+$ T cells in their lungs as compared with mock-treated MR1$^{-/-}$ mice; importantly, the elevated number of activated CD4$^+$ T cells in MR1$^{-/-}$ adoptive transfer recipients was not significantly different from WT mice. Thus, Mo-DCs are an important DC subset

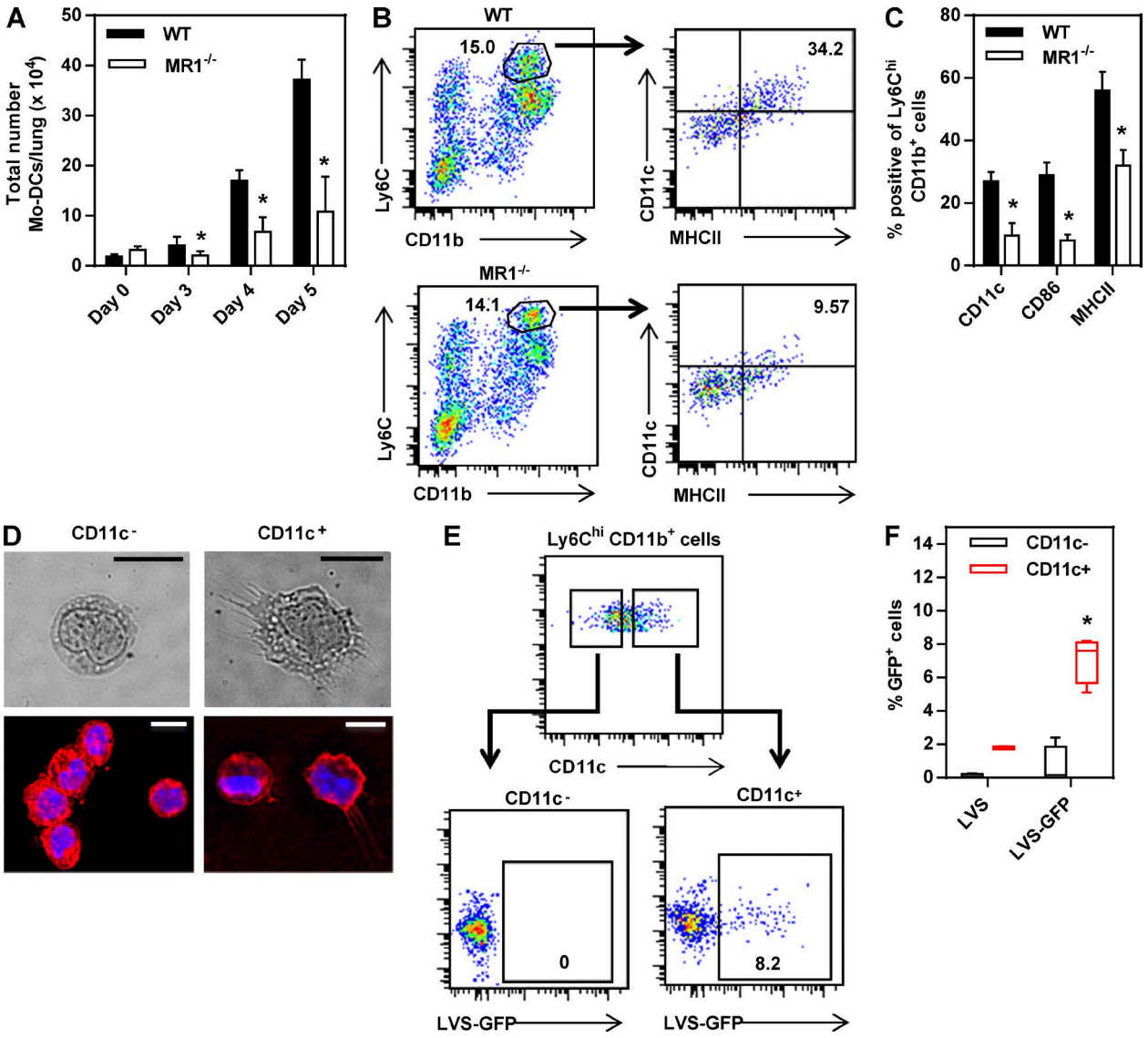

Figure 4. **Differentiation of inflammatory monocytes into Mo-DCs is impaired in the lungs of MR1$^{-/-}$ mice after i.n. *F. tularensis* LVS infection.** Wild-type C57BL/6 and MR1$^{-/-}$ mice were infected with a sublethal dose of 2 × 10^2 CFU *F. tularensis* i.n. LVS, and (A) total lung cells were harvested at the indicated time points to evaluate the presence of Mo-DCs (Ly6C^{hi} CD11b$^+$ MHCII$^+$ CD11c$^+$ cells). Data are representative of three independent experiments (n = 5 mice per group), and are the mean ± SEM. *, P < 0.05, compared with LVS-infected WT mice at the same time point. (B) Flow cytometry analyses of Mo-DCs in the lungs of WT and MR1$^{-/-}$ mice on day 4 after infection. Representative dot plots are shown. (C) Analysis of CD11c, CD86, and MHCII expression by Ly6C^{hi} CD11b$^+$ cells in the lungs of mice on day 4 after i.n. LVS infection. Data are representative of three independent experiments (n = 5 mice per group), and are the mean ± SEM. *, P < 0.05, compared with LVS-infected WT mice at the same time point. (D) Cytospin preparations of CD11c$^-$ and CD11c$^+$ inflammatory monocytes (Ly6C^{hi} CD11b$^+$ cells) purified from the lungs of LVS-infected mice on day 4 after infection by fluorescence-activated cell sorting and examined by light microscopy (top) or confocal microscopy (bottom) using wheat germ agglutinin-Alexa Fluor 594–conjugated membrane stain (red) and Hoechst nuclear stain (blue). Bars, 10 µm. Lung cells were pooled from 10 mice for flow sorting, and data are representative of three independent experiments. (E) WT mice were infected i.n. with LVS-GFP or LVS, and GFP$^+$ cells were evaluated in CD11c$^-$ and CD11c$^+$ inflammatory monocytes (Ly6C^{hi} CD11b$^+$ cells) by flow cytometry on day 4 after infection. Representative dot plots are shown. (F) Quantification of the percentage of GFP$^+$ CD11c$^-$ and CD11c$^+$ inflammatory monocytes (Ly6C^{hi} CD11b$^+$ cells) in the lungs of mice on day 4 after infection with either LVS-GFP or LVS (negative GFP control). Data are representative of three independent experiments (n = 5 mice per group) and are the mean ± SEM. *, P < 0.05, compared with LVS-infected WT mice at the same time point. Data were analyzed via one-way ANOVA followed by the Student-Newman-Keuls multiple stepwise comparison.

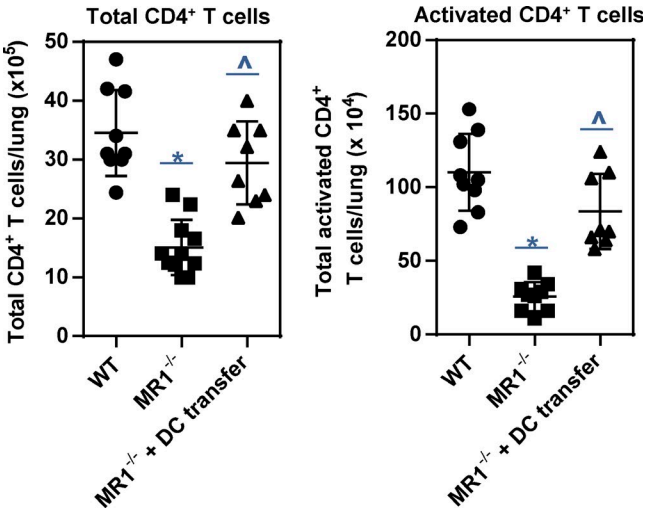

Figure 5. **Adoptive transfer of Mo-DCs to MR1$^{-/-}$ mice rescues their impairment in the accumulation of activated CD4$^+$ T cells in the lungs after i.n. *F. tularensis* LVS infection.** Wild-type C57BL/6 mice were infected with a sublethal dose of 2 × 10^2 CFU *F. tularensis* i.n. LVS, and Mo-DCs were purified from the lungs on day 4 after infection by fluorescence-activated cell sorting using the gating scheme shown in Fig. 1 A, gate R3. 10^6 Mo-DCs were transferred i.v. to MR1$^{-/-}$ mice on day 3 after i.n. LVS infection. Lungs were harvested from WT mice, MR1$^{-/-}$ mice, and MR1$^{-/-}$ adoptive transfer recipients and the total numbers of CD4$^+$ T cells and activated (CD69$^+$ CD44$^+$) CD4$^+$ T cells were quantified by flow cytometry on day 8 after i.n. LVS infection. Data are representative of three independent experiments, and are the mean ± SEM. *, $P < 0.05$, compared with LVS-infected WT mice. ^, $P < 0.05$, compared with LVS-infected MR1$^{-/-}$ mice. Data were analyzed via one-way ANOVA, followed by the Student-Newman-Keuls multiple stepwise comparison.

that rescue the defect in activated CD4$^+$ T cell recruitment to the lungs of MR1$^{-/-}$ mice during i.n. LVS infection.

MAIT cells directly stimulate the differentiation of bone marrow–derived monocyte precursors into Mo-DCs

We next sought to determine the mechanism behind the impaired differentiation of inflammatory monocytes into Mo-DCs in MR1$^{-/-}$ mice. Because either IFN-γ or GM-CSF can induce bone marrow monocyte differentiation into Mo-DCs in vitro (Serbina and Pamer, 2006; Osterholzer et al., 2009), we examined the effect of these two cytokines on the capacity of MR1$^{-/-}$ bone marrow precursors (Ly6C^{hi} CD11b$^+$ monocytes) to differentiate into Mo-DCs in vitro. We purified Ly6C^{hi} CD11b$^+$ monocytes from the bone marrow of WT and MR1$^{-/-}$ mice, and cultured them in the presence of either recombinant IFN-γ or GM-CSF. As shown in Fig. 6, cells exposed to either IFN-γ or GM-CSF significantly up-regulated CD11c and MHC class II expression (Fig. 6, A and B). Of note, GM-CSF stimulated higher level CD11c expression than IFN-γ (Fig. 6 A), and promoted accumulation of higher numbers of these cells than IFN-γ, which is consistent with the ability of GM-CSF to act as a growth factor (Fig. 6 C). Equivalent numbers of WT and MR1$^{-/-}$ monocytes coexpressed CD11c and MHC II after cytokine treatment (Figs. 6, A and B), suggesting that Ly6C^{hi} CD11b$^+$ monocytes in MR1$^{-/-}$ mice are not functionally blocked for differentiation, and indicating that the tissues of these mice lack the appropriate signals to encourage differentiation.

To evaluate whether MAIT cells directly stimulate inflammatory monocyte differentiation, Ly6C^{hi} CD11b$^+$ monocytes purified from naive WT bone marrow were co-cultured with total Thy1.2$^+$ cells isolated from transgenic mice that exclusively express the canonical MAIT cell Vα19-Jα33 TCRα chain (Vα19iTgCα$^{-/-}$MR1$^{+/+}$ mice). LVS-infected macrophages from WT mice were included in the cultures as a source of antigen-presenting cells to facilitate MAIT cell activation. After 3 d of culture, the Ly6C^{hi} CD11b$^+$ monocytes were assessed for changes in CD11c and MHC II coexpression (gating of Ly6C^{hi} CD11b$^+$ monocytes is shown in Fig. S1). Few Ly6C^{hi} CD11b$^+$ monocytes expressed CD11c and MHCII after 3 d of culture with LVS-infected macrophages (12 ± 1% MHCII$^+$CD11c$^+$ monocytes; Fig. 7 A, first panel). In contrast, Ly6C^{hi} CD11b$^+$ monocytes significantly up-regulated CD11c and MHC class II expression when Vα19iTg Thy1.2$^+$ cells were included in the cultures, increasing to a mean of 61.5 ± 1% MHCII$^+$CD11c$^+$ monocytes (Fig. 7 A, second panel). Because Thy1.2$^+$ cells isolated from Vα19iTg mice may contain additional T cell subsets that are not MAIT cells, we compared the ability of Thy1.2$^+$ cells isolated from naive WT C57BL/6 mice and Vα19iTg mice to drive monocyte differentiation in the presence of LVS-infected macrophages. As before, Vα19iTg Thy1.2$^+$ cells promoted monocyte MHC class II and CD11c up-regulation, whereas cultures containing naive WT C57BL/6 Thy1.2$^+$ cells were not significantly different from cultures lacking T cells (Fig. 7 B), demonstrating that other non-MAIT cell Thy1.2$^+$ cell subsets present in naive spleens do not significantly affect monocyte differentiation in the co-cultures. To assess the role of cognate antigen recognition in this process, Ly6C^{hi} CD11b$^+$ monocytes were purified from the bone marrow of naive MR1$^{-/-}$ mice and co-cultured with Vα19iTg Thy1.2$^+$ cells in the presence of LVS-infected MR1$^{-/-}$ macrophages. As shown in Fig. 7 C, the absence of MR1 had no effect on up-regulation of MHCII and CD11c by monocytes as compared with cultures containing WT monocytes and WT macrophages. Similar results were observed for WT monocytes and WT macrophages cultured with Vα19iTg Thy1.2$^+$ cells in the presence of a blocking anti-MR1 antibody (unpublished data). Thus, the ability of Vα19iTg Thy1.2$^+$ cells to drive monocyte differentiation in the cultures was independent of MR1.

Because recombinant IFN-γ and GM-CSF directly stimulated the differentiation of Ly6C^{hi} CD11b$^+$ bone marrow monocytes in vitro (Fig. 6), we investigated whether these cytokines were responsible for monocyte differentiation in the Vα19iTg Thy1.2$^+$ cell cultures. Both IFN-γ and GM-CSF were detected in the supernatants of cultures containing Vα19iTg Thy1.2$^+$ cells and LVS-infected macrophages, but not in cultures that lacked Vα19iTg Thy1.2$^+$ cells, demonstrating that

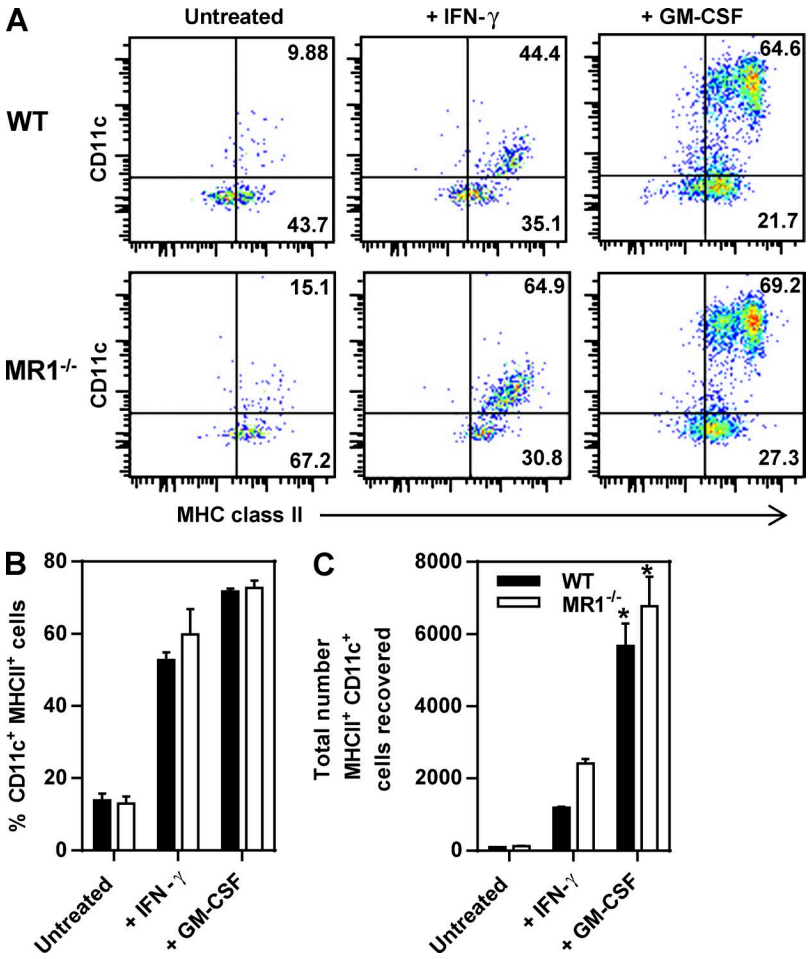

Figure 6. **Bone marrow monocytes from MR1$^{-/-}$ mice do not exhibit a defect in differentiation into MHCII$^+$ CD11c$^+$ cells in response to recombinant cytokines in vitro.** Monocytes (Ly6C^{hi} CD11b$^+$ cells) were purified from the bone marrow of naive WT and MR1$^{-/-}$ mice by fluorescence-activated cell sorting and cultured for 3 d in the presence of recombinant IFN-γ or GM-CSF (100 ng/ml), then assessed for coexpression of MHCII and CD11c by flow cytometry. Representative flow cytometry dot plots are shown (A). The percentage (B) and total number (C) of MHCII$^+$ CD11c$^+$ monocytes is shown. Bone marrow cells were pooled and sorted from 50 mice; data includes values ± SEM from three replicates, and is representative of three independent experiments. *, $P < 0.01$, compared with IFN-γ–treated cells. Data were analyzed via one-way ANOVA, followed by the Student-Newman-Keuls multiple stepwise comparison.

Vα19iTg Thy1.2$^+$ cells are likely the source of both cytokines (Fig. 7 D). Addition of neutralizing anti–IFN-γ antibodies to the cultures did not significantly impact the total number of differentiated monocytes expressing both MHCII and CD11c (Fig. 7 A, third panel). In contrast, addition of neutralizing anti–GM-CSF antibodies significantly inhibited monocyte differentiation, resulting in a lower number of differentiated monocytes (Fig. 7 A, fourth panel). Simultaneous addition of both anti–IFN-γ and anti–GM-CSF Abs to the cultures had no additional impact on monocyte differentiation (unpublished data). Thus, GM-CSF is the dominant cytokine driving monocyte differentiation in the in vitro co-cultures. Overall, these data show that MAIT cells can stimulate the differentiation of bone marrow–derived Ly6C^{hi} CD11b$^+$ monocytes in a GM-CSF–dependent and MR1-independent manner.

MAIT cell–dependent production of GM-CSF is required for early differentiation of inflammatory monocytes into Mo-DCs in the lungs

Because our results revealed that MAIT cell–derived GM-CSF contributed to the differentiation of bone marrow Ly6C^{hi} CD11b$^+$ cells into Mo-DCs in vitro, we next sought to examine the role of GM-CSF during i.n. LVS infection in vivo. GM-CSF production significantly increased in the lungs of WT mice during the first 4 d of infection (Fig. 8 A); in contrast, GM-CSF in the lungs of MR1$^{-/-}$ mice on days 2 and 3 after infection was significantly reduced as compared with WT mice, and was not significantly different from naive mice. By day 4 after and thereafter, GM-CSF levels in the lungs of MR1$^{-/-}$ mice were not significantly different from the levels present in the lungs of WT mice. Because M-CSF can also drive inflammatory monocyte differentiation in several inflammation models in vivo (Greter et al., 2012), we similarly examined the levels of M-CSF in the lungs of mice during i.n. LVS infection (Fig. 8 A). M-CSF levels in the lungs did not significantly increase as compared with naive mice during the first 5 d of infection, and no significant differences were observed between WT and MR1$^{-/-}$ mice. Overall, these results demonstrate that MAIT cells are required for initial early GM-CSF production, but not M-CSF production, in the lungs after i.n. LVS infection.

We next examined the levels of expression of the M-CSF receptor (CD115) and GM-CSF receptor (CSF2-Rα) on inflammatory monocytes infiltrating the lungs during i.n. LVS infection. As a positive control for CD115 expression, we examined Ly6C^{hi} CD11b$^+$ cells in the bone marrow of

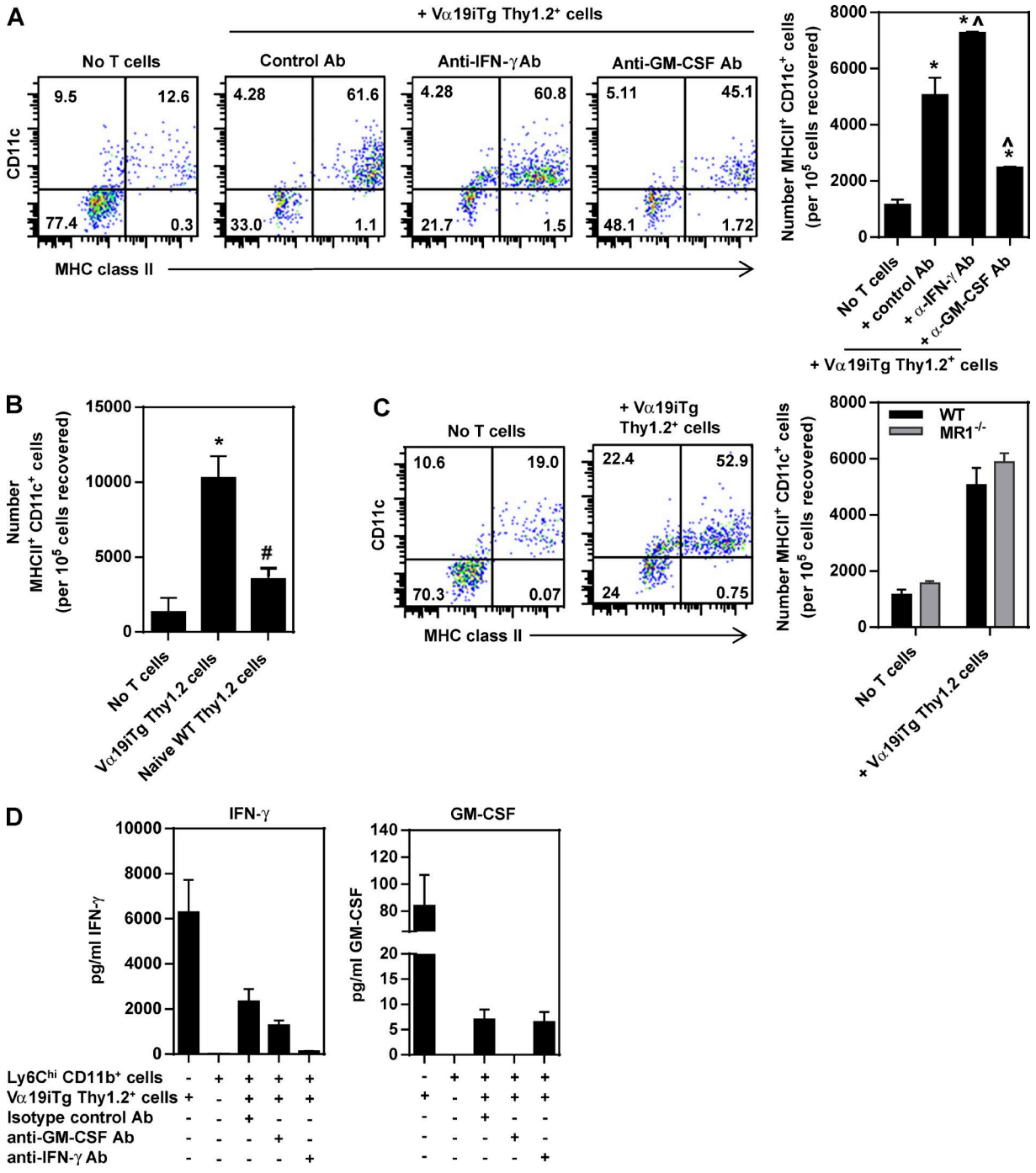

Figure 7. **Vα19iTg T cells promote the differentiation of bone marrow monocytes into MHCII+CD11c+ cells in a GM-CSF–dependent manner in vitro.** Monocytes (Ly6C^{hi} CD11b$^+$ cells) were purified from the bone marrow of naive WT and MR1$^{-/-}$ mice by fluorescence-activated cell sorting and cultured for 3 d in the presence of MAIT cells and LVS-infected macrophages, then assessed for coexpression of MHCII and CD11c by flow cytometry. Thy1.2$^+$ cells purified from transgenic Vα19iTgCα$^{-/-}$MR1$^{+/+}$ mice were the source of MAIT cells. In some cases, as indicated, neutralizing antibodies or isotype control antibodies were added to the cultures at the time of addition of purified MAIT cells. In A, representative flow cytometry dot plots and the number of MHCII$^+$ CD11c$^+$ monocytes are shown for cultures containing WT bone marrow monocytes and LVS-infected WT macrophages in the presence or absence of Vα19iTg Thy1.2$^+$ cells. In B, the number of MHCII$^+$ CD11c$^+$ monocytes are shown for cultures containing WT bone marrow monocytes, LVS-infected WT macrophages, and either Vα19iTg Thy1.2$^+$ cells or naive WT C57BL/6 Thy1.2$^+$ cells. In C, representative flow cytometry dot plots of MHCII$^+$ CD11c$^+$ monocytes are shown for cultures containing MR1$^{-/-}$ bone marrow monocytes, LVS-infected MR1$^{-/-}$ macrophages, and Vα19iTg Thy1.2$^+$ cells. Graph of the numbers of MHCII$^+$ CD11c$^+$ monocytes obtained from MR1$^{-/-}$ cultures as compared with WT cultures (note that A and B are all from the same representative experiment). In D,

mice on day 4 after i.n. LVS infection, and found they were highly positive for CD115 expression (Fig. 8 B); however, Ly6C^{hi} CD11b^{+} inflammatory monocytes in the lungs of WT mice on day 4 after i.n. LVS infection expressed very low levels of CD115. In contrast, the majority of inflammatory monocytes were highly positive for CSF2-Rα, indicating that these cells have the capacity to respond to GM-CSF during i.n. LVS infection.

We next investigated whether GM-CSF is required for the differentiation of inflammatory monocytes into Mo-DCs during i.n. LVS infection in vivo. Because mice genetically deficient for GM-CSF (or its receptor) develop alveolar proteinosis (Trapnell et al., 2003), we instead used neutralizing antibodies to deplete mice of GM-CSF. Although the total numbers of Ly6C^{hi} CD11b^{+} inflammatory monocytes in the lungs on day 4 after infection were not significantly affected by GM-CSF depletion (Fig. 8 C), the number of these cells coexpressing CD11c and MHCII was significantly lower in GM-CSF–depleted mice as compared with WT mice, and not significantly different from MR1$^{-/-}$ mice (Fig. 8, D and E). Isotype control antibody-treated and untreated WT mice showed no significant differences in inflammatory monocyte and Mo-DC accumulation in the lungs on day 4 after i.n. LVS infection (unpublished data). Overall, these data demonstrate that GM-CSF is required for the differentiation of inflammatory monocytes into Mo-DCs, and further show that MAIT cells are necessary for early GM-CSF production in the lungs of mice after i.n. LVS infection.

DISCUSSION

Mo-DCs transiently accumulate in inflamed tissues and lymph nodes during infection (Nakano et al., 2009). These cells are not present in the steady state, but differentiate from recently recruited CCR2^{+} inflammatory monocytes (Hohl et al., 2009; Osterholzer et al., 2009; Greter et al., 2012). Consistent with the model that Mo-DCs mediate adaptive immunity, these cells stimulate robust Th1 responses in vitro, and mice lacking CCR2 exhibit impaired T cell responses during infection (Peters et al., 2001; Nakano et al., 2009). However, thus far little is known about the cell types required to drive Mo-DC differentiation. Because MAIT cells recognize a microbial molecular pattern, possess a memory phenotype, and are present in peripheral tissues (Rahimpour et al., 2015), they are in an ideal position to influence early innate immune responses. Here, we show that MR1$^{-/-}$ mice recruited normal numbers of inflammatory monocytes to the lungs, but these cells were delayed in their differentiation into Mo-DCs during *F. tularensis* LVS pulmonary infection. Further, adoptive transfer of Mo-DCs to infected MR1$^{-/-}$ mice rescued a defect in the recruitment of activated CD4^{+} T cells to the lungs in these mice. Finally, we show that MAIT cells promote monocyte differentiation into Mo-DCs in a GM-CSF–dependent manner in vitro, are required for early GM-CSF production in the lungs in vivo, and that GM-CSF is necessary for Mo-DC accumulation during LVS pulmonary infection. Overall, these results demonstrate that MAIT cells have a critical role in directing the differentiation of recently recruited inflammatory monocytes into Mo-DCs, and that the paucity of these cells impacts later adaptive immune responses.

Because adoptive transfer of Mo-DCs to MR1$^{-/-}$ mice restored their defect in activated CD4^{+} T cell accumulation in the lungs during infection, we further examined this population to better understand their function. Our Mo-DC population expressed a variety of markers that were consistent with lung Mo-DCs identified in other pulmonary infection models, such as CD64 and CD172α (Greter et al., 2012). These cells were largely positive for the co-stimulatory markers CD40 and CD86, and intracellular LVS was detected in these cells (5–8%). This percentage of infected cells is within the range reported for infected Mo-DCs in the *L. major* (5%) and *A. fumigatus* (17%) models (León et al., 2007; Hohl et al., 2009). A significant percentage of Mo-DCs expressed CCR7 (~13%), which is found on mature DCs and coordinates the migration of these cells to secondary lymphoid tissues (Förster et al., 1999). Indeed, Bar-Haim et al. (2008) identified a similar CD11b^{hi} CD11c^{int} DC population in the lungs of mice during i.n. LVS infection that migrated to local lymph nodes and harbored intracellular bacteria. Importantly, during *L. major* skin infection and *A. fumigatus* pulmonary infection, CCR2^{+} Ly6C^{hi} CD11b^{+} monocytes were recruited to the inflamed tissues, where they differentiated into Mo-DCs locally, acquired antigen, and migrated to regional lymph nodes (León et al., 2007; Hohl et al., 2009). Collectively, these data suggest that a subset of the Mo-DC population found in the lungs of LVS-infected mice may transport antigen to draining lymph nodes and promote T cell activation. However, it remains to be determined whether the role of Mo-DCs in this process involves lymph node migration, or whether these cells have other important in situ lung functions such as cytokine and chemokine production. Indeed, Mo-DCs have been shown to produce several inflammatory mediators, including IL-1β, IL-6, IL-12, TNF, and various chemokines (León et al., 2007; Zhan et al., 2010; Ko et al., 2014; Croxford et al., 2015). It also remains to be determined whether the reduced numbers of Mo-DCs in the lungs of MR1$^{-/-}$ mice impacts bacterial growth control. Because Mo-DCs promote activated

IFN-γ and GM-CSF in the supernatants of cultures containing WT bone marrow monocytes, LVS-infected WT macrophages, and Vα19iTg Thy1.2^{+} cells after 3 d are shown. Bone marrow cells were pooled from 50 mice per experiment; data includes values ± SEM from two pooled experiments, each containing two replicate samples, and is representative of five independent experiments. *, $P < 0.01$, compared with No T cells. ^, $P < 0.01$, compared with +Vα19i Thy1.2 cells + control Ab. #, $P < 0.01$, compared with +Vα19i Thy1.2 cells. Data were analyzed via one-way ANOVA followed by the Student-Newman-Keuls multiple stepwise comparison.

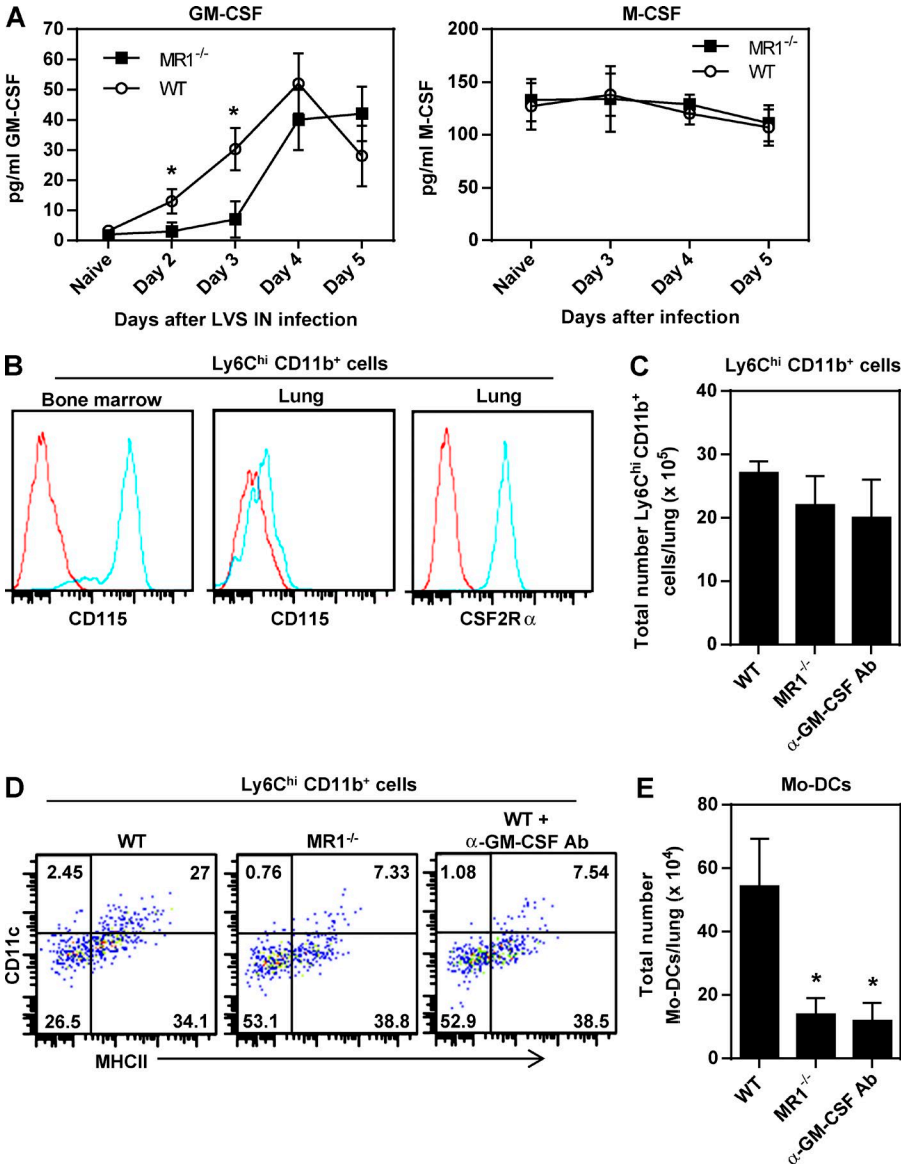

Figure 8. **MAIT cells are required for early GM-CSF production in the lungs after i.n. *F. tularensis* LVS infection.** Wild-type C57BL/6 and MR1$^{-/-}$ mice were infected with a sublethal dose of 2 × 10^2 CFU *F. tularensis* i.n. LVS, and (A) the levels of GM-CSF and M-CSF were determined in lung homogenates during the first 5 d of infection (n = 5 mice per group). (B) Expression of CD115 and CSF2Rα by inflammatory monocytes (Ly6C^{hi} CD11b$^+$ cells) in the bone marrow and lungs on day 4 after i.n. LVS infection. Red line, fluorescence minus one control; blue line, staining by the indicated antibody. (C) Enumeration of the total number of Ly6C^{hi} CD11b$^+$ inflammatory monocytes in the lungs of WT, MR1$^{-/-}$, and GM-CSF–depleted WT mice on day 4 after i.n. LVS infection. (D) Representative flow cytometry dot plots of Mo-DC accumulation in the lungs of WT, MR1$^{-/-}$, and GM-CSF–depleted WT mice on day 4 after i.n. LVS infection. (E) Enumeration of the total number of Mo-DCs in the lungs of WT, MR1$^{-/-}$, and GM-CSF–depleted WT mice on day 4 after i.n. LVS infection. Data are representative of four independent experiments (n = 5 mice per group), and are the mean ± SEM *, P < 0.01, compared with WT mice. Data were analyzed via one-way ANOVA followed by the Student-Newman-Keuls multiple stepwise comparison.

CD4$^+$ T cell accumulation, it is possible that they indirectly affect bacterial clearance. However, MAIT cells also express several products that can contribute to LVS growth control, such as production of IFN-γ, TNF, Granzyme B, and IL-17A (Gold et al., 2010; Dusseaux et al., 2011; Meierovics et al., 2013; Kurioka et al., 2015), suggesting that their ability to promote Mo-DC accumulation is only one of many mechanisms that can influence the outcome of infection.

The delayed accumulation of Mo-DCs in the lungs of infected MR1$^{-/-}$ mice indicates that MAIT cells have either a direct or indirect role in stimulating inflammatory monocyte differentiation into Mo-DCs. Using in vitro cultures, we found that MAIT cells directly stimulated differentiation of purified Ly6C^{hi} CD11b$^+$ bone marrow monocytes, a process largely driven by MAIT cell–dependent GM-CSF. Our source of MAIT cells for these studies were Vα19iTgCα$^{-/-}$MR1$^{+/+}$ mice, which exclusively express the canonical TRAV1-TRAJ33 TCRα gene sequence and are highly enriched for MAIT cells. Typically, such studies would use Vα19iTg Cα$^{-/-}$MR1$^{-/-}$ mice as a negative control, because in theory these mice lack MAIT cells due to the absence of MR1. However, it was recently shown that Vα19iTg Cα$^{-/-}$MR1$^{-/-}$ mice contain a large population of MAIT-like MR1 tetramer-reactive T cells (Sakala et al., 2015). These "MAIT-like" cells were functionally responsive to synthetic vitamin B2 antigens, although they were much less reactive than MAIT cells from Vα19iTg Cα$^{-/-}$MR1$^{+/+}$ mice. Because the α1 and α2 domains of MR1 share sequence and structural similarity with MHC class I, it has been speculated that the MAIT-like T cells found in Vα19iTg Cα$^{-/-}$MR1$^{-/-}$ mice are selected by a weak cross-reaction with MHC class Ia (Sakala et al., 2015).

Thus, in lieu of this control strain, we showed that resident splenic T cells from naive WT mice, which contain very few MAIT cells (0.06% of total $\alpha\beta^+$ T cells; Rahimpour et al., 2015), lack the capacity to drive monocyte differentiation. In further support of our findings, both human and murine MAIT cells have previously been shown to produce GM-CSF (Lepore et al., 2014; Cui et al., 2015; Rahimpour et al., 2015). Our data are also consistent with the observation that NKT cell clones directed human monocytes to differentiate into DCs in a GM-CSF– and IL-13–dependent manner (Hegde et al., 2007). For NKT cells, this process required antigen recognition via CD1d. In contrast, we found that MAIT cells stimulated monocyte differentiation in vitro in a MR1-independent manner. Because several studies have demonstrated that cytokines, such as IL-18 and IL-12, can drive MAIT cell IFN-γ–production in the absence of cognate antigen (Chua et al., 2012; Ussher et al., 2014; Sakala et al., 2015), the existence of a cytokine-driven, MR1-independent route for MAIT cell GM-CSF production is feasible. Whether cognate antigen recognition is required for MAIT cells to direct monocyte differentiation during in vivo infection remains to be determined.

Although it is broadly accepted that GM-CSF promotes the differentiation of monocytes into DCs in vitro (Scheicher et al., 1992; Osterholzer et al., 2009; Helft et al., 2015), the in vivo role for GM-CSF in this process remains controversial. GM-CSF was required for the accumulation of Mo-DCs in antigen-induced peritonitis and LPS-induced lung inflammation, as well as in acute inflammatory arthritis (Campbell et al., 2011; Louis et al., 2015). In contrast, GM-CSF was dispensable for Mo-DC differentiation in thioglycollate-induced peritonitis and LPS-induced spleen inflammation (Campbell et al., 2011), as well as several infection models (Greter et al., 2012; Ko et al., 2014). Recent studies by Greter et al. (2012) identified a critical role for M-CSF in Mo-DC development during LPS-induced spleen inflammation and i.n. influenza infection. These cumulative data suggest that the requirement for GM-CSF or M-CSF in promoting Mo-DC accumulation depends on the nature of the inflammatory stimulus. In the LVS pulmonary infection model, we found that few inflammatory monocytes and Mo-DCs present in the lungs expressed the M-CSF receptor (CD115), but were almost entirely positive for the GM-CSF receptor. Sköld and Behar (2008) similarly noted a lack of high CD115 expression by myeloid subsets in the lungs during *M. tuberculosis* pulmonary infection. We further found that GM-CSF, but not M-CSF, significantly increased in the lungs of WT mice early after i.n. LVS infection, and that this increase in pulmonary GM-CSF was delayed in $MR1^{-/-}$ mice. Collectively, these data implicated GM-CSF, rather than M-CSF, in the delayed differentiation of Mo-DCs in $MR1^{-/-}$ mice during LVS infection. This is additionally supported by our finding that GM-CSF–deficient mice exhibited normal accumulation of inflammatory monocytes, but impaired differentiation of monocytes into Mo-DCs. Our results are consistent with the *C. neoformans* pulmonary infection model, whereby GM-CSF–deficient mice exhibited impaired accumulation of Mo-DCs in the lungs (Chen et al., 2016). Overall, our data demonstrate that GM-CSF promotes monocyte differentiation into Mo-DCs during LVS pulmonary infection, and that MAIT cells are essential for the initial production of GM-CSF during the early stages of infection.

Because the MAIT cell population in murine lungs during the first week of LVS infection is small, and we currently lack specific markers to distinguish MAIT cells from other T cells, and we cannot conclusively state whether MAIT cells produce GM-CSF in vivo themselves or induce GM-CSF production by other cells in the lungs. However, Rahimpour et al. (2015) used a MR1 tetramer to demonstrate that MAIT cells in naive mouse lungs predominantly expressed the transcription factor RORγt, and were potent producers of IL-17. Notably, ROR response elements have been identified in the *csf2* promoter region, and RORγt drove GM-CSF gene expression in Th17 cells in an IL-23–dependent manner during autoimmune neuroinflammation (Codarri et al., 2011). This suggests that the $ROR\gamma t^+$ MAIT cell population present in naive mouse lungs has the potential to produce GM-CSF if exposed to the correct cytokine environment. Indeed, MAIT cells circulating in the mucosal tissues of naive mice may be ideally programmed to produce GM-CSF upon microbial exposure.

Our data support a model whereby MAIT cell–dependent GM-CSF production directs Mo-DC differentiation during the early stages of LVS pulmonary infection, and that this influences the magnitude of $CD4^+$ T cell responses. Several lines of evidence suggest that enhancing GM-CSF levels during vaccination promotes vaccine-induced immune responses. For example, administration of GM-CSF DNA in conjunction with several different DNA vaccines enhanced both cellular and humoral immune responses (Geissler et al., 1997; Barouch et al., 2002; Yoon et al., 2006). Similarly, i.n. administration of a GM-CSF–expressing BCG vaccine to mice increased migration of activated $CD4^+$ T cells to the lungs and amplified BCG-induced protection against pulmonary TB challenge (Nambiar et al., 2010). However, because overexpression of GM-CSF in the lungs impaired protective immunity to *M. tuberculosis* infection (Szeliga et al., 2008), these data suggest that GM-CSF levels must be carefully regulated to function as an adjuvant. Importantly, compounds that encourage MAIT cell activation may function as effective adjuvants by inducing MAIT cells to promote early immune responses such as GM-CSF production, which have the potential to amplify critical elements of adaptive immunity.

MATERIALS AND METHODS

Bacteria

F. tularensis LVS (ATCC) was grown and frozen as previously described (Fortier et al., 1991). Viable bacteria were quantified by plating serial dilutions on supplemented Mueller-Hinton agar plates.

Animals and infections

Male and female specific pathogen–free CCR2$^{-/-}$ mice and C57BL/6J mice were purchased from The Jackson Laboratory. MR1$^{-/-}$ mice and Vα19iTgCα$^{-/-}$MR1$^{+/+}$ transgenic mice (Kawachi et al., 2006) were obtained from Ted Hansen (Washington University in St. Louis [WUSTL], St. Louis, MO) and bred at CBER/FDA. Vα19iTgCα$^{-/-}$MR1$^{+/+}$ transgenic mice exclusively express the canonical TCR Vα of mouse MAIT cells. Animals were housed in a barrier environment at CBER/FDA, and procedures were performed according to approved protocols under the FDA Animal Care and Use Committee guidelines. i.n. infections were performed by delivering 2 × 10^2 LVS CFU in a volume of 25 µl/naris to anesthetized mice. Bacteria were diluted in PBS (Cambrex) containing <0.01 ng/ml endotoxin.

Preparation of single-cell suspensions from lungs

To prepare lung cells for flow cytometry, the lungs were excised after perfusion through the right heart ventricle with a solution of DMEM containing 2% FBS, collagenase (0.72 mg/ml) and DNase (10 U/ml). Harvested lungs were subjected to pressure disruption, followed by incubation for 20 min at 37°C in 5% CO_2. Released cells were filtered through a Filtra-bag (Lab Plas), subjected to ACK lysis, and passed through a 40-µm filter. Live cells were enumerated on a hemocytometer after dilution in Trypan blue.

Flow cytometry analyses

Single-cell suspensions from lungs were prepared as described in the previous section. Cells were stained for a panel of murine cell surface markers and analyzed using a Fortessa X-20 (BD) and FlowJo software (Tree Star). Antibody clones used included RM4-5 (anti-CD4), 53–6.7 (anti-CD8α), and H57-597 (anti-TCRβ chain), all obtained from BD. In addition, H1.2F3 (anti-CD69), IM7 (anti-CD44), XMG-6 (anti-IFN-γ), N418 (anti-CD11c), M5/114.15.2 (anti-IA/IE), HK1.4 (anti-Ly6C), 1A8 (anti-Ly6G), M1/70 (anti-CD11b), 2E7 (anti-CD103), P84 (anti-CD172α), X54-5/7.1 (anti-CD64), BM8 (anti-F4/80), M1/69 (anti-CD24), RA3-6B2 (anti-B220), 4B12 (anti-CCR7), MP1-22E9 (anti-CSFR2α), AFS98 (anti-CD115), 323 (anti-CD40), and GL-1 (anti-CD86) were obtained from BioLegend. Clone 475301 (anti-CCR2) was obtained from R&D Systems. Live/Dead Near IR stain was obtained from Life Technologies and included in all staining protocols. Optimal antibody concentrations were determined in separate experiments, and appropriate fluorochrome-labeled isotype control antibodies used throughout. In all cases, cells were first gated on singlets (FSC-W vs. FSC-A or -H) and live cells (Live/Dead Near IR negative) before further analyses.

In vitro culture of bone marrow Ly6C^{hi} CD11b^{+} monocytes with MAIT cells

Bone marrow–derived macrophages were used as antigen-presenting cells for the in vitro co-cultures. Complete DMEM (cDMEM) was used in all experiments, and consisted of DMEM + 10% fetal bovine serum (Hyclone) + 10% L-glutamine (Lonza) + 10% nonessential amino acids (Lonza) + 10% Hepes (Lonza). BMMØ were cultured as previously described, using BMMØ medium (cDMEM + L-929 supernatant supplement; Cowley and Elkins, 2003). Cells were plated at 5 × 10^5 cells per well in 96-well plates in BMMØ medium supplemented with 50 µg/ml gentamycin (Life Technologies) and incubated at 37°C in 5% CO_2. After 1 d of incubation, the medium was replaced with antibiotic-free BMMØ medium, and the cells were incubated for an additional 6 d at 37°C in 5% CO_2. The medium was replaced with fresh, gentamycin-free BMMØ medium every 2 d during the 7-d incubation. After the 7-d culture period, the BMMØ concentration was estimated to be 2 × 10^6 cells/well. BMMØ were then infected with *F. tularensis* LVS at a multiplicity of infection (MOI) of 1:1 (bacterium-to-BMMØ ratio) in cDMEM. LVS was coincubated with BMMØ at 37°C in 5% CO_2 for 2 h, and then washed three times with phosphate-buffered saline (PBS; Lonza). The monolayers were incubated for 1 h in cDMEM supplemented with 50 µg/ml gentamicin to eliminate extracellular bacteria. The BMMØ were washed an additional three times with PBS, followed by addition of cDMEM and purified MAIT cells at a ratio of one purified MAIT cell per two macrophages.

Vα19iTgCα$^{-/-}$MR1$^{+/+}$ mice were used as source of naive splenic total Thy1.2^{+} MAIT cells for co-culture with LVS-infected BMMØs and Ly6C^{hi} CD11b^{+} bone marrow monocytes. Total Thy1.2^{+} T cells were purified from Vα19iTgCα$^{-/-}$MR1$^{+/+}$ or WT C57BL/6 mouse spleens using a Thy1.2^{+} Dynabead cell enrichment column (Life Technologies), according to the manufacturer's recommendations. Where indicated, anti-MR1 Ab clone 26.5 (Ted Hansen, WUSTL, St. Louis, MO) was added to BMMØ cultures at a concentration of 25 µg/ml 1 h before adding MAIT cells. Other antibodies were added at a concentration of 25 µg/ml (anti–IFN-γ; BD; and anti–GM-CSF; BioLegend). In all cases, antibodies were added at the time of addition of MAIT cells to the cultures, and remained present for the entire 3-d co-culture period.

To obtain Ly6C^{hi} CD11b^{+} bone marrow monocytes, CD11b^{+} bone marrow cells from naive WT or MR1$^{-/-}$ mice were first enriched using anti-CD11b beads (STEM CELL Technologies) according to the manufacturer's instructions. Cells positive for Ly6C^{hi} and CD11b were flow sorted using the FACSAria and Fusion instruments (BD). Monocyte post-sort purity was >98%. These cells were added to the co-cultures at a concentration of 5 × 10^5 cells/well. The co-cultures were incubated at 37°C in 5% CO_2 in cDMEM for 3 d before collection of supernatants and nonadherent cells for further analyses. To identify bone marrow monocytes in the cultures, nonadherent cells were gated to identify CCR2^{+} Ly6C^{hi} CD11b^{+} cells. Differentiation of these cells was evaluated based on coexpression of MHCII and CD11c.

In vitro culture of bone marrow monocytes with recombinant cytokines

Ly6C^{hi} CD11b^{+} bone marrow monocytes were flow sorted from WT and MR1$^{-/-}$ mice as described above. These cells were added to wells at a concentration of 2×10^5 cells/well in the presence of either 100 ng/ml recombinant GM-CSF or IFN-γ (eBioscience) in cDMEM. The cultures were incubated at 37°C in 5% CO_2 in cDMEM for 3 d before collection of nonadherent cells for analyses. Nonadherent cells were first gated to identify CCR2^{+}, Ly6C^{hi}, and CD11b^{+} cells. Differentiation of these cells was evaluated based on coexpression of MHCII and CD11c.

In vivo depletion of GM-CSF

Antibodies for in vivo depletion used the anti–GM-CSF Ab clone MP1-22E9 (BioLegend) or the rat IgG_{2a} isotype control Ab clone RTK2758 (BioLegend), and were administered to mice intraperitoneally at a concentration of 0.5 mg/injection on days 0 and +1 relative to i.n. LVS infection (day 0).

Adoptive transfer experiments

WT C57BL/6J mice were infected with 2×10^2 CFU i.n. LVS. On day 4 after infection, lungs were harvested and single-cell suspensions were prepared as described above. To obtain purified Mo-DCs/CD11b^{+} DCs, lung cells were stained with the appropriate antibody cocktail, using a previously described gating scheme (Hohl et al., 2009), and flow cytometry-sorted for MHCII^{+} CD11c^{+} CD11b^{hi} and CD103^{-} cells using the FACSAria and Fusion instruments (BD). Mo-DC post-sort purity was >97%. 10^6 purified Mo-DCs were transferred intravenously to infected MR1$^{-/-}$ mice (previously given 2×10^2 i.n. LVS) late on day 3 after infection. The time for adoptive transfer was selected to allow the transferred Mo-DCs to recover and migrate to the appropriate locations at a time when we typically first observe Mo-DCs accumulating in the lungs of WT mice (Fig. 1). On day 8 after infection, the lungs of these mice were assessed for the presence of activated TCRβ^{+}CD4^{+} T cells, which were identified as CD69^{+} CD44^{hi}.

Microscopy

CD11b^{+} DCs were flow sorted from WT mice on day 4 after i.n. LVS infection as described above. Cytospin preparations of the sorted cells were examined by light microscopy. To obtain purified inflammatory monocytes and Mo-DCs on day 4 after i.n. LVS infection, lungs were harvested and single-cell suspensions were prepared as described above. Cells were stained with the appropriate antibody cocktail and sorted using flow cytometry to obtain cells that were Ly6C^{hi} CD11b^{+} CD11c^{-} (inflammatory monocytes) and cells that were Ly6C^{hi} CD11b^{+} CD11c^{+} (Mo-DCs). Cytospin preparations of sorted cells were examined by light microscopy or confocal microscopy. Cells assessed by confocal microscopy were first stained using Hoechst nuclear dye (Life Technologies) and wheat germ agglutinin-Alexa Fluor 594-conjugated membrane dye (Life Technologies) according to the manufacturer's instructions.

Quantitation of cytokines in culture supernatants and lung homogenates

Culture supernatants and lung homogenates were assayed by Luminex assay for GM-CSF (Affymetrix/eBioscience) and ELISA (Abcam) for M-CSF, according to the manufacturer's instructions.

Statistical analyses

All experiments were performed using five mice per experimental group unless otherwise stated in the figure legend, and repeated at least three times to assess reproducibility. Data were analyzed via one-way ANOVA followed by the Student-Newman-Keuls multiple stepwise comparison (for experiments with more than two experimental groups).

Online supplemental material

Fig. S1 shows the flow cytometry gating used to examine bone marrow monocytes co-cultured with Vα19iTg Thy1.2^{+} cells.

ACKNOWLEDGMENTS

The authors are grateful to Dr. Ted Hansen for providing the anti-MR1 Ab clone 26.5, as well as the MR1$^{-/-}$ and Vα19i transgenic mice, Kazuyo Takeda for confocal microscopy, as well as Dr. Ronald Rabin for helpful review and discussion.

This work was funded by internal Center for Biologics Evaluation and Research/Food and Drug Administration (U.S. government) operating funds.

The authors declare no competing financial interests.

Submitted: 4 May 2016
Revised: 14 July 2016
Accepted: 29 September 2016

REFERENCES

Bar-Haim, E., O. Gat, G. Markel, H. Cohen, A. Shafferman, and B. Velan. 2008. Interrelationship between dendritic cell trafficking and Francisella tularensis dissemination following airway infection. *PLoS Pathog.* 4:e1000211. http://dx.doi.org/10.1371/journal.ppat.1000211

Barouch, D.H., S. Santra, K. Tenner-Racz, P. Racz, M.J. Kuroda, J.E. Schmitz, S.S. Jackson, M.A. Lifton, D.C. Freed, H.C. Perry, et al. 2002. Potent CD4+ T cell responses elicited by a bicistronic HIV-1 DNA vaccine expressing gp120 and GM-CSF. *J. Immunol.* 168:562–568. http://dx.doi.org/10.4049/jimmunol.168.2.562

Bosschaerts, T., M. Guilliams, B. Stijlemans, Y. Morias, D. Engel, F. Tacke, M. Hérin, P. De Baetselier, and A. Beschin. 2010. Tip-DC development during parasitic infection is regulated by IL-10 and requires CCL2/CCR2, IFN-gamma and MyD88 signaling. *PLoS Pathog.* 6:e1001045. http://dx.doi.org/10.1371/journal.ppat.1001045

Campbell, I.K., A. van Nieuwenhuijze, E. Segura, K. O'Donnell, E. Coghill, M. Hommel, S. Gerondakis, J.A. Villadangos, and I.P. Wicks. 2011. Differentiation of inflammatory dendritic cells is mediated by NF-κB1-dependent GM-CSF production in CD4 T cells. *J. Immunol.* 186:5468–5477. http://dx.doi.org/10.4049/jimmunol.1002923

Chen, G.H., S. Teitz-Tennenbaum, L.M. Neal, B.J. Murdock, A.N. Malachowski, A.J. Dils, M.A. Olszewski, and J.J. Osterholzer. 2016. Local GM-CSF-dependent differentiation and activation of pulmonary dendritic cells and macrophages protect against progressive cryptococcal lung infection in mice. *J. Immunol.* 196:1810–1821. http://dx.doi.org/10.4049/jimmunol.1501512

Chong, S.Z., K.L. Wong, G. Lin, C.M. Yang, S.C. Wong, V. Angeli, P.A. Macary, and D.M. Kemeny. 2011. Human $CD8^+$ T cells drive Th1 responses through the differentiation of TNF/iNOS-producing dendritic cells. *Eur. J. Immunol.* 41:1639–1651. http://dx.doi.org/10.1002/eji.201041022

Chua, W.J., S.M. Truscott, C.S. Eickhoff, A. Blazevic, D.F. Hoft, and T.H. Hansen. 2012. Polyclonal mucosa-associated invariant T cells have unique innate functions in bacterial infection. *Infect. Immun.* 80:3256–3267. http://dx.doi.org/10.1128/IAI.00279-12

Codarri, L., G. Gyülvészi, V. Tosevski, L. Hesske, A. Fontana, L. Magnenat, T. Suter, and B. Becher. 2011. RORγt drives production of the cytokine GM-CSF in helper T cells, which is essential for the effector phase of autoimmune neuroinflammation. *Nat. Immunol.* 12:560–567. http://dx.doi.org/10.1038/ni.2027

Cowley, S.C. 2014. MAIT cells and pathogen defense. *Cell. Mol. Life Sci.* 71:4831–4840. http://dx.doi.org/10.1007/s00018-014-1708-y

Cowley, S.C., and K.L. Elkins. 2003. Multiple T cell subsets control *Francisella tularensis* LVS intracellular growth without stimulation through macrophage interferon gamma receptors. *J. Exp. Med.* 198:379–389. http://dx.doi.org/10.1084/jem.20030687

Croxford, A.L., M. Lanzinger, F.J. Hartmann, B. Schreiner, F. Mair, P. Pelczar, B.E. Clausen, S. Jung, M. Greter, and B. Becher. 2015. The Cytokine GM-CSF drives the inflammatory signature of $CCR2^+$ monocytes and licenses autoimmunity. *Immunity.* 43:502–514. http://dx.doi.org/10.1016/j.immuni.2015.08.010

Cui, Y., K. Franciszkiewicz, Y.K. Mburu, S. Mondot, L. Le Bourhis, V. Premel, E. Martin, A. Kachaner, L. Duban, M.A. Ingersoll, et al. 2015. Mucosal-associated invariant T cell-rich congenic mouse strain allows functional evaluation. *J. Clin. Invest.* 125:4171–4185. http://dx.doi.org/10.1172/JCI82424

Dennis, D.T., T.V. Inglesby, D.A. Henderson, J.G. Bartlett, M.S. Ascher, E. Eitzen, A.D. Fine, A.M. Friedlander, J. Hauer, M. Layton, et al. Working Group on Civilian Biodefense. 2001. Tularemia as a biological weapon: medical and public health management. *JAMA.* 285:2763–2773. http://dx.doi.org/10.1001/jama.285.21.2763

Dusseaux, M., E. Martin, N. Serriari, I. Péguillet, V. Premel, D. Louis, M. Milder, L. Le Bourhis, C. Soudais, E. Treiner, and O. Lantz. 2011. Human MAIT cells are xenobiotic-resistant, tissue-targeted, CD161hi IL-17-secreting T cells. *Blood.* 117:1250–1259. http://dx.doi.org/10.1182/blood-2010-08-303339

Elkins, K.L., S.C. Cowley, and C.M. Bosio. 2003. Innate and adaptive immune responses to an intracellular bacterium, *Francisella tularensis* live vaccine strain. *Microbes Infect.* 5:135–142. http://dx.doi.org/10.1016/S1286-4579(02)00084-9

Ellis, J., P.C. Oyston, M. Green, and R.W. Titball. 2002. Tularemia. *Clin. Microbiol. Rev.* 15:631–646. http://dx.doi.org/10.1128/CMR.15.4.631-646.2002

Espinosa, V., A. Jhingran, O. Dutta, S. Kasahara, R. Donnelly, P. Du, J. Rosenfeld, I. Leiner, C.C. Chen, Y. Ron, et al. 2014. Inflammatory monocytes orchestrate innate antifungal immunity in the lung. *PLoS Pathog.* 10:e1003940. http://dx.doi.org/10.1371/journal.ppat.1003940

Förster, R., A. Schubel, D. Breitfeld, E. Kremmer, I. Renner-Müller, E. Wolf, and M. Lipp. 1999. CCR7 coordinates the primary immune response by establishing functional microenvironments in secondary lymphoid organs. *Cell.* 99:23–33. http://dx.doi.org/10.1016/S0092-8674(00)80059-8

Fortier, A.H., M.V. Slayter, R. Ziemba, M.S. Meltzer, and C.A. Nacy. 1991. Live vaccine strain of *Francisella tularensis*: infection and immunity in mice. *Infect. Immun.* 59:2922–2928.

Geissler, M., A. Gesien, K. Tokushige, and J.R. Wands. 1997. Enhancement of cellular and humoral immune responses to hepatitis C virus core protein using DNA-based vaccines augmented with cytokine-expressing plasmids. *J. Immunol.* 158:1231–1237.

Georgel, P., M. Radosavljevic, C. Macquin, and S. Bahram. 2011. The non-conventional MHC class I MR1 molecule controls infection by *Klebsiella pneumoniae* in mice. *Mol. Immunol.* 48:769–775. http://dx.doi.org/10.1016/j.molimm.2010.12.002

Gold, M.C., and D.M. Lewinsohn. 2013. Co-dependents: MR1-restricted MAIT cells and their antimicrobial function. *Nat. Rev. Microbiol.* 11:14–19. http://dx.doi.org/10.1038/nrmicro2918

Gold, M.C., S. Cerri, S. Smyk-Pearson, M.E. Cansler, T.M. Vogt, J. Delepine, E. Winata, G.M. Swarbrick, W.J. Chua, Y.Y. Yu, et al. 2010. Human mucosal associated invariant T cells detect bacterially infected cells. *PLoS Biol.* 8:e1000407. http://dx.doi.org/10.1371/journal.pbio.1000407

Greter, M., J. Helft, A. Chow, D. Hashimoto, A. Mortha, J. Agudo-Cantero, M. Bogunovic, E.L. Gautier, J. Miller, M. Leboeuf, et al. 2012. GM-CSF controls nonlymphoid tissue dendritic cell homeostasis but is dispensable for the differentiation of inflammatory dendritic cells. *Immunity.* 36:1031–1046. http://dx.doi.org/10.1016/j.immuni.2012.03.027

Guilliams, M., K. Movahedi, T. Bosschaerts, T. VandenDriessche, M.K. Chuah, M. Hérin, A. Acosta-Sanchez, L. Ma, M. Moser, J.A. Van Ginderachter, et al. 2009. IL-10 dampens TNF/inducible nitric oxide synthase-producing dendritic cell-mediated pathogenicity during parasitic infection. *J. Immunol.* 182:1107–1118. http://dx.doi.org/10.4049/jimmunol.182.2.1107

Guilliams, M., B.N. Lambrecht, and H. Hammad. 2013. Division of labor between lung dendritic cells and macrophages in the defense against pulmonary infections. *Mucosal Immunol.* 6:464–473. http://dx.doi.org/10.1038/mi.2013.14

Hegde, S., X. Chen, J.M. Keaton, F. Reddington, G.S. Besra, and J.E. Gumperz. 2007. NKT cells direct monocytes into a DC differentiation pathway. *J. Leukoc. Biol.* 81:1224–1235. http://dx.doi.org/10.1189/jlb.1206718

Helft, J., J. Böttcher, P. Chakravarty, S. Zelenay, J. Huotari, B.U. Schraml, D. Goubau, and C. Reis e Sousa. 2015. GM-CSF Mouse Bone Marrow Cultures Comprise a Heterogeneous Population of CD11c(+)MHC II(+) Macrophages and Dendritic Cells. *Immunity.* 42:1197–1211. http://dx.doi.org/10.1016/j.immuni.2015.05.018

Hohl, T.M., A. Rivera, L. Lipuma, A. Gallegos, C. Shi, M. Mack, and E.G. Pamer. 2009. Inflammatory monocytes facilitate adaptive CD4 T cell responses during respiratory fungal infection. *Cell Host Microbe.* 6:470–481. http://dx.doi.org/10.1016/j.chom.2009.10.007

Huang, S., S. Gilfillan, M. Cella, M.J. Miley, O. Lantz, L. Lybarger, D.H. Fremont, and T.H. Hansen. 2005. Evidence for MR1 antigen presentation to mucosal-associated invariant T cells. *J. Biol. Chem.* 280:21183–21193. http://dx.doi.org/10.1074/jbc.M501087200

Huang, S., E. Martin, S. Kim, L. Yu, C. Soudais, D.H. Fremont, O. Lantz, and T.H. Hansen. 2009. MR1 antigen presentation to mucosal-associated invariant T cells was highly conserved in evolution. *Proc. Natl. Acad. Sci. USA.* 106:8290–8295. http://dx.doi.org/10.1073/pnas.0903196106

Kang, S.J., H.E. Liang, B. Reizis, and R.M. Locksley. 2008. Regulation of hierarchical clustering and activation of innate immune cells by dendritic cells. *Immunity.* 29:819–833. http://dx.doi.org/10.1016/j.immuni.2008.09.017

Kawachi, I., J. Maldonado, C. Strader, and S. Gilfillan. 2006. MR1-restricted V alpha 19i mucosal-associated invariant T cells are innate T cells in the gut lamina propria that provide a rapid and diverse cytokine response. *J. Immunol.* 176:1618–1627. http://dx.doi.org/10.4049/jimmunol.176.3.1618

Kjer-Nielsen, L., O. Patel, A.J. Corbett, J. Le Nours, B. Meehan, L. Liu, M. Bhati, Z. Chen, L. Kostenko, R. Reantragoon, et al. 2012. MR1 presents microbial vitamin B metabolites to MAIT cells. *Nature.* 491:717–723.

Ko, H.J., J.L. Brady, V. Ryg-Cornejo, D.S. Hansen, D. Vremec, K. Shortman, Y. Zhan, and A.M. Lew. 2014. GM-CSF-responsive monocyte-derived dendritic cells are pivotal in Th17 pathogenesis. *J. Immunol.* 192:2202–2209. http://dx.doi.org/10.4049/jimmunol.1302040

Kurioka, A., J.E. Ussher, C. Cosgrove, C. Clough, J.R. Fergusson, K. Smith, Y.H. Kang, L.J. Walker, T.H. Hansen, C.B. Willberg, and P. Klenerman. 2015. MAIT cells are licensed through granzyme exchange to kill bacterially sensitized targets. *Mucosal Immunol.* 8:429–440. http://dx.doi.org/10.1038/mi.2014.81

Le Bourhis, L., M. Dusseaux, A. Bohineust, S. Bessoles, E. Martin, V. Premel, M. Coré, D. Sleurs, N.E. Serriari, E. Treiner, et al. 2013. MAIT cells detect and efficiently lyse bacterially-infected epithelial cells. *PLoS Pathog.* 9:e1003681. http://dx.doi.org/10.1371/journal.ppat.1003681

León, B., M. López-Bravo, and C. Ardavín. 2007. Monocyte-derived dendritic cells formed at the infection site control the induction of protective T helper 1 responses against *Leishmania*. *Immunity.* 26:519–531. http://dx.doi.org/10.1016/j.immuni.2007.01.017

Lepore, M., A. Kalinichenko, A. Colone, B. Paleja, A. Singhal, A. Tschumi, B. Lee, M. Poidinger, F. Zolezzi, L. Quagliata, et al. 2014. Parallel T-cell cloning and deep sequencing of human MAIT cells reveal stable oligoclonal TCRβ repertoire. *Nat. Commun.* 5:3866.

Lin, K.L., Y. Suzuki, H. Nakano, E. Ramsburg, and M.D. Gunn. 2008. CCR2+ monocyte-derived dendritic cells and exudate macrophages produce influenza-induced pulmonary immune pathology and mortality. *J. Immunol.* 180:2562–2572. http://dx.doi.org/10.4049/jimmunol.180.4.2562

Louis, C., A.D. Cook, D. Lacey, A.J. Fleetwood, R. Vlahos, G.P. Anderson, and J.A. Hamilton. 2015. Specific contributions of CSF-1 and GM-CSF to the dynamics of the mononuclear phagocyte system. *J. Immunol.* 195:134–144. http://dx.doi.org/10.4049/jimmunol.1500369

Meierovics, A., W.J. Yankelevich, and S.C. Cowley. 2013. MAIT cells are critical for optimal mucosal immune responses during in vivo pulmonary bacterial infection. *Proc. Natl. Acad. Sci. USA.* 110:E3119–E3128. http://dx.doi.org/10.1073/pnas.1302799110

Nakano, H., K.L. Lin, M. Yanagita, C. Charbonneau, D.N. Cook, T. Kakiuchi, and M.D. Gunn. 2009. Blood-derived inflammatory dendritic cells in lymph nodes stimulate acute T helper type 1 immune responses. *Nat. Immunol.* 10:394–402. http://dx.doi.org/10.1038/ni.1707

Nambiar, J.K., A.A. Ryan, C.U. Kong, W.J. Britton, and J.A. Triccas. 2010. Modulation of pulmonary DC function by vaccine-encoded GM-CSF enhances protective immunity against Mycobacterium tuberculosis infection. *Eur. J. Immunol.* 40:153–161. http://dx.doi.org/10.1002/eji.200939665

Osterholzer, J.J., G.H. Chen, M.A. Olszewski, J.L. Curtis, G.B. Huffnagle, and G.B. Toews. 2009. Accumulation of CD11b+ lung dendritic cells in response to fungal infection results from the CCR2-mediated recruitment and differentiation of Ly-6Chigh monocytes. *J. Immunol.* 183:8044–8053. http://dx.doi.org/10.4049/jimmunol.0902823

Peters, W., H.M. Scott, H.F. Chambers, J.L. Flynn, I.F. Charo, and J.D. Ernst. 2001. Chemokine receptor 2 serves an early and essential role in resistance to Mycobacterium tuberculosis. *Proc. Natl. Acad. Sci. USA.* 98:7958–7963. http://dx.doi.org/10.1073/pnas.131207398

Peters, W., J.G. Cyster, M. Mack, D. Schlöndorff, A.J. Wolf, J.D. Ernst, and I.F. Charo. 2004. CCR2-dependent trafficking of F4/80dim macrophages and CD11cdim/intermediate dendritic cells is crucial for T cell recruitment to lungs infected with Mycobacterium tuberculosis. *J. Immunol.* 172:7647–7653. http://dx.doi.org/10.4049/jimmunol.172.12.7647

Rahimpour, A., H.F. Koay, A. Enders, R. Clanchy, S.B. Eckle, B. Meehan, Z. Chen, B. Whittle, L. Liu, D.P. Fairlie, et al. 2015. Identification of phenotypically and functionally heterogeneous mouse mucosal-associated invariant T cells using MR1 tetramers. *J. Exp. Med.* 212:1095–1108. http://dx.doi.org/10.1084/jem.20142110

Sakala, I.G., L. Kjer-Nielsen, C.S. Eickhoff, X. Wang, A. Blazevic, L. Liu, D.P. Fairlie, J. Rossjohn, J. McCluskey, D.H. Fremont, et al. 2015. Functional heterogeneity and antimycobacterial effects of mouse mucosal-associated invariant T cells specific for riboflavin metabolites. *J. Immunol.* 195:587–601. http://dx.doi.org/10.4049/jimmunol.1402545

Scheicher, C., M. Mehlig, R. Zecher, and K. Reske. 1992. Dendritic cells from mouse bone marrow: in vitro differentiation using low doses of recombinant granulocyte-macrophage colony-stimulating factor. *J. Immunol. Methods.* 154:253–264. http://dx.doi.org/10.1016/0022-1759(92)90199-4

Serbina, N.V., and E.G. Pamer. 2006. Monocyte emigration from bone marrow during bacterial infection requires signals mediated by chemokine receptor CCR2. *Nat. Immunol.* 7:311–317. http://dx.doi.org/10.1038/ni1309

Serbina, N.V., T.P. Salazar-Mather, C.A. Biron, W.A. Kuziel, and E.G. Pamer. 2003. TNF/iNOS-producing dendritic cells mediate innate immune defense against bacterial infection. *Immunity.* 19:59–70. http://dx.doi.org/10.1016/S1074-7613(03)00171-7

Serbina, N.V., T. Jia, T.M. Hohl, and E.G. Pamer. 2008. Monocyte-mediated defense against microbial pathogens. *Annu. Rev. Immunol.* 26:421–452. http://dx.doi.org/10.1146/annurev.immunol.26.021607.090326

Shi, C., and E.G. Pamer. 2011. Monocyte recruitment during infection and inflammation. *Nat. Rev. Immunol.* 11:762–774. http://dx.doi.org/10.1038/nri3070

Sköld, M., and S.M. Behar. 2008. Tuberculosis triggers a tissue-dependent program of differentiation and acquisition of effector functions by circulating monocytes. *J. Immunol.* 181:6349–6360. http://dx.doi.org/10.4049/jimmunol.181.9.6349

Sung, S.S., S.M. Fu, C.E. Rose Jr., F. Gaskin, S.T. Ju, and S.R. Beaty. 2006. A major lung CD103 (alphaE)-beta7 integrin-positive epithelial dendritic cell population expressing Langerin and tight junction proteins. *J. Immunol.* 176:2161–2172. http://dx.doi.org/10.4049/jimmunol.176.4.2161

Szeliga, J., D.S. Daniel, C.H. Yang, Z. Sever-Chroneos, C. Jagannath, and Z.C. Chroneos. 2008. Granulocyte-macrophage colony stimulating factor-mediated innate responses in tuberculosis. *Tuberculosis (Edinb.).* 88:7–20. http://dx.doi.org/10.1016/j.tube.2007.08.009

Tezuka, H., Y. Abe, M. Iwata, H. Takeuchi, H. Ishikawa, M. Matsushita, T. Shiohara, S. Akira, and T. Ohteki. 2007. Regulation of IgA production by naturally occurring TNF/iNOS-producing dendritic cells. *Nature.* 448:929–933. http://dx.doi.org/10.1038/nature06033

Trapnell, B.C., J.A. Whitsett, and K. Nakata. 2003. Pulmonary alveolar proteinosis. *N. Engl. J. Med.* 349:2527–2539. http://dx.doi.org/10.1056/NEJMra023226

Ussher, J.E., M. Bilton, E. Attwod, J. Shadwell, R. Richardson, C. de Lara, E. Mettke, A. Kurioka, T.H. Hansen, P. Klenerman, and C.B. Willberg. 2014. $CD161^{++}$ $CD8^{+}$ T cells, including the MAIT cell subset, are specifically activated by IL-12+IL-18 in a TCR-independent manner. *Eur. J. Immunol.* 44:195–203. http://dx.doi.org/10.1002/eji.201343509

Wüthrich, M., K. Ersland, T. Sullivan, K. Galles, and B.S. Klein. 2012. Fungi subvert vaccine T cell priming at the respiratory mucosa by preventing chemokine-induced influx of inflammatory monocytes. *Immunity.* 36:680–692. http://dx.doi.org/10.1016/j.immuni.2012.02.015

Yee, D., T.R. Rhinehart-Jones, and K.L. Elkins. 1996. Loss of either $CD4^{+}$ or $CD8^{+}$ T cells does not affect the magnitude of protective immunity to an intracellular pathogen, *Francisella tularensis* strain LVS. *J. Immunol.* 157:5042–5048.

Yoon, H.A., A.G. Aleyas, J.A. George, S.O. Park, Y.W. Han, J.H. Lee, J.G. Cho, and S.K. Eo. 2006. Cytokine GM-CSF genetic adjuvant facilitates prophylactic DNA vaccine against pseudorabies virus through enhanced immune responses. *Microbiol. Immunol.* 50:83–92. http://dx.doi.org/10.1111/j.1348-0421.2006.tb03773.x

Zhan, Y., Y. Xu, S. Seah, J.L. Brady, E.M. Carrington, C. Cheers, B.A. Croker, L. Wu, J.A. Villadangos, and A.M. Lew. 2010. Resident and monocyte-derived dendritic cells become dominant IL-12 producers under different conditions and signaling pathways. *J. Immunol.* 185:2125–2133. http://dx.doi.org/10.4049/jimmunol.0903793